Nonequilibrium Energy Profiles for a Class of 1-D Models

Jean-Pierre Eckmann[1,2] **and Lai-Sang Young**[3]

[1]Département de Physique Théorique, Université de Genève,
[2]Section de Mathématiques, Université de Genève,
[3]Courant Institute for Mathematical Sciences, New York University

Abstract

As a paradigm for heat conduction in 1 dimension, we propose a class of models represented by chains of identical cells, each one of which containing an energy storage device called a "tank". Energy exchange among tanks is mediated by tracer particles, which are injected at characteristic temperatures and rates from heat baths at the two ends of the chain. For stochastic and Hamiltonian models of this type, we develop a theory that allows one to derive rigorously – under physically natural assumptions – macroscopic equations for quantities related to heat transport, including mean energy profiles and tracer densities. Concrete examples are treated for illustration, and the validity of the Fourier Law in the present context is discussed.

Contents

JPE is partially supported by the Fonds National Suisse.
LSY is partially supported by NSF Grant #0100538.

1 Introduction

Heat conduction in solids has been a subject of intensive study ever since Fourier's pioneering work. An interesting issue is the derivation of macroscopic conduction laws from the microscopic dynamics describing the solid. A genuinely realistic model of the solid would involve considerations of quantum mechanics, radiation and other phenomena. In this paper, we address a simpler set of questions, viewing solids that are effectively 1-dimensional as modeled by chains of classical Hamiltonian systems in which heat transport is mediated by tracer particles. Coupling the two ends of the chain to unequal tracer-heat reservoirs and allowing the system to settle down to a nonequilibrium steady state, we study the distribution of energy, heat flux, and tracer flux in this context.

We introduce in this paper a class of models that can be seen as an abstraction of certain types of mechanical models. These models are simple enough to be amenable to analysis, and complex enough to have fairly rich dynamics. They have in common the following basic set of characteristics: Each model is made up of an array of identical cells that are linearly ordered. Energy is carried by two types of agents: storage receptacles (called "tanks") that are fixed in place, and tracer particles that move about. Direct energy exchange is permitted only between tracers and tanks. The two ends of the chain are coupled to infinite reservoirs that emit tracer particles at characteristic rates and characteristic temperatures; they also absorb those tracers that reach them. To allow for a broad range of examples, we do not specify the rules of interaction between tracers and tanks. All the rules considered in this paper have a Hamiltonian character, involving the kinetic energy of tracers. Formally they may be stochastic or purely dynamical, resulting in what we will refer to as *stochastic* and *Hamiltonian models*.

Via the models in this class, we seek to clarify the relation among several aspects of conduction, including the role of conservation laws, their relation to the dynamics within individual cells, and the notion of "local temperature". We propose a simple recipe for deducing various macroscopic profiles from local rules (see Sect. 2.2). Our recipe is generic; it does not depend on specific characteristics of the system. When the local rules are sufficiently simple, it produces explicit formulas that depend on exactly 4 parameters: the temperatures and rates of tracer injection at the left and right ends of the chain.

For demonstration purposes, we carry out this proposed program for a few examples. Our main stochastic example, dubbed the "random-halves model", is particularly simple: A clock rings with rate proportional to $\sqrt{x}$ where x is the (kinetic) energy of the tracer; at the clock, energy exchange between tracer and tank takes place; and the rule of exchange consists simply of pooling the two energies together and randomly dividing – in an unbiased way – the total energy into two parts. Our main Hamiltonian example is a variant of the model studied in [17, 12]. Here the role of the "tank" is played by a rotating disk nailed down at its center, and stored energy is ω^2 where ω is the angular velocity of the disk. Explicit formulas for the profiles in question are correctly predicted in all examples.

In terms of methodology, this paper has a theory part and a simulations part. The theory part is rigorous in the sense that all points that are not proven are isolated and stated explicitly as "assumptions" (see the next paragraph). It also serves to elucidate the relation between various concepts regardless of the extent to which the assumed properties hold. Simulations are used to verify these properties for the models considered.

Our main assumption is in the direction of local thermodynamic equilibrium. For our stochastic models, a proof of this property seems within reach though technically involved (see *e.g.* [5, 22, 10] and [11]); no known techniques are available for Hamiltonian systems. Extra assumptions pertaining to ergodicity and mixing issues are needed for our Hamiltonian models. It is easy to "improve ergodicity" via model design, harder to mathematically eliminate the possibility of all (small) invariant regions. In the absence of perfect mixing within cells, actual profiles show small deviations from those predicted for the ideal case.

In summary, we introduce in this paper a relatively tractable class of models that can be seen as paradigms for heat conduction, and put forth a program which – under natural assumptions – takes one from the microscopic dynamics of a system to its phenomenological laws of conduction.

2 Main Ideas

2.1 General setup

The models considered in this paper – both stochastic and Hamiltonian – have in common a basic set of characteristics which we now describe.

There is a finite, linearly ordered collection of *sites* or *cells* labeled $1, 2, \ldots, N$. In isolation, *i.e.*, when the chain is not in contact with any external heat source, the system is driven by the interaction between two distinct types of energy-carrying objects:

- Objects of the first kind are *fixed in place*, and there is exactly one at each site. These objects play the role of storage facility, and serve at the same time to mark the energy level at fixed locations. For brevity and for lack of a better word, let us call them energy **tanks**. Each tank holds a finite amount of energy at any one point in time; it is not to be confused with an infinite reservoir. We will refer to the energy in the tank at site i as the **stored energy** at site i.
- The second type of objects are moving particles called **tracers**. Each tracer carries with it a finite amount of energy, and moves from site to site. For definiteness, we assume that from site i, it can go only to sites $i \pm 1$.

With regard to **microscopic dynamics**, the following is assumed: When a tracer is at site i, it may interact – possibly multiple times – with the tank at that site. In each interaction, the two energies are pooled together and redistributed, so that energy is conserved in each interaction. The times of interaction and manner of redistribution are determined by the microscopic laws of the system, which depend solely on conditions within that site. These laws determine also the exit times of the tracers and their next locations. *A priori* there is no limit to how many tracers are allowed at each site. We stress that this tracer-tank interaction is the only type of interaction permitted: the tanks at different sites can communicate with each other only via the tracers, and the tracers do not "see" each other directly.

All *stochastic* models considered in this paper are Markovian. Typically in stochastic rules of interaction, energy exchanges occur when exponential clocks ring, and energy is redistributed according to probability distributions. In *Hamiltonian* models, tracers are usually embodied by real-life moving particles, and energy exchanges usually involve some types of collisions.

The two ends of the chain above are coupled to two **heat baths**, which are infinite reservoirs emitting tracers at characteristic temperature (and also absorbing them). It is sometimes convenient to think of them as located at sites 0 and $N+1$. The two baths inject tracers into the system according to certain rules (to be described). Tracers at site 1 or N can exit the system; when they do so, they are absorbed by the baths. The actions of the two baths are assumed to be independent of each other and independent of the state of the chain. The left bath is set at temperature $T_{\rm L}$; the energies of the tracers it injects into the system are *iid* with a law depending on the model. These tracers are injected at exponential rates, with mean $\varrho_{\rm L}$. Similarly the bath on the right is set at temperature $T_{\rm R}$ and injects tracers into the system at rate $\varrho_{\rm R}$.

To allow for a broad spectrum of possibilities, we have deliberately left unspecified (i) the rules of interaction between tracers and tanks, and (ii) the coupling to heat baths, *i.e.*, the energy distribution of the injected tracers. (Readers who wish to see concrete examples immediately can skip ahead with no difficulty to Sects. 3.1 and 4.1, where two examples are presented.) We stress that once (i) and (ii) are chosen, and the 4 parameters $T_{\rm L}, T_{\rm R}, \varrho_{\rm L}$ and $\varrho_{\rm R}$ are set, then all is determined: the system will evolve on its own, and there is to be no other intervention of any kind.

Remark 2.1 Our approach can be viewed as that of a grand-canonical ensemble, since we fix the rates at which tracers are injected into the system (which indirectly determine the density and energy flux at steady state). An alternate setup would be one in which the density of tracers is given, with particles being replaced upon exit. In this alternate setup, the 4 natural extensive variables would be the temperatures $T_{\rm L}$ and $T_{\rm R}$, the density of tracers (mean number of tracers per cell) and the mean energy flux. For definiteness, we will adhere to our original formulation.

We now introduce the **quantities of interest**. For fixed N, let μ_N denote the invariant measure corresponding to the unique steady state of the N-chain (assuming there is a unique steady state). The word "mean" below refers to averages with respect to μ_N. The main quantities of interest in this paper are

- s_i = mean stored energy at site i ;
- e_i = mean energy of individual tracers at site i ;
- k_i = mean number of tracers at site i ;
- E_i = mean total energy at site i, including stored energy and the energies of all tracers present.

For simplicity, we will refer to e_i as *tracer energy* and E_i as *total-cell energy*.

We are primarily interested in the **profiles** of these quantities, *i.e.*, in the functions $i \mapsto s_i, e_i, k_i$ and E_i as $N \to \infty$ *with the temperatures and injection rates of the baths held fixed*. More precisely, we fix $T_{\rm L}, T_{\rm R}, \varrho_{\rm L}$ and $\varrho_{\rm R}$. Then spacing $\{1, 2, \ldots, N\}$ evenly along the unit interval $[0, 1]$ and letting $N \to \infty$, the finite-volume profiles $i \mapsto s_i, e_i, k_i, E_i$ give rise to functions $\xi \mapsto s(\xi), e(\xi), k(\xi), E(\xi)$, $\xi \in [0, 1]$. It is these functions that we seek to predict given the microscopic rules that define a system.

2.2 Proposed program: from local rules to global profiles

We fix N, $T_{\rm L}, T_{\rm R}, \varrho_{\rm L}$ and $\varrho_{\rm R}$, and consider an N-chain with these parameters. To determine the profiles in Sect. 2.1, we distinguish between the following two kinds of information:

(a) cell-to-cell traffic, and

(b) statistical information pertaining to the dynamics within individual cells.

In (a), we regard the cells as black boxes, and observe only what goes in and what comes out. Where left-right exit distributions are known, standard arguments balancing energy and tracer fluxes give easily the mean number of tracers and energy transported from site to site. While these numbers are indicative of the internal states of the cells (for example, high-energy tracers emerging from a cell suggests higher temperatures inside), the profiles we seek depend on more intricate relations than these numbers alone would tell us.

We turn therefore to (b). Our very naïve idea is to study a *single cell*, and to bring to bear on chains of arbitrary length the information so obtained. We propose the following plan of action:

(i) Consider a single cell plugged to two heat baths (one on its left, the other on its right), both of which are at temperature T and have injection rate ϱ, T and ϱ being arbitrary. Finding the invariant measure $\mu^{T,\varrho}$ describing the state of the cell in this equilibrium situation is, in general, relatively simple compared to finding μ_N.

(ii) Suppose the measure $\mu^{T,\varrho}$ has been found. We then look at an N-chain with $T_{\rm L} = T_{\rm R} = T$ and $\varrho_{\rm L} = \varrho_{\rm R} = \varrho$, and verify that the marginals at site i of the invariant measure μ_N are equal to $\mu^{T,\varrho}$. (By the marginal at site i, we refer to the measure obtained by integrating out all variables pertaining to all sites $\neq i$.)

(iii) Once the family $\{\mu^{T,\varrho}\}$ is found and (ii) verified, we *assume* that the structure common to the $\mu^{T,\varrho}$ passes to all marginals of μ_N as $N \to \infty$ even when $(T_{\rm L}, \varrho_{\rm L}) \neq (T_{\rm R}, \varrho_{\rm R})$. More precisely, for all $\xi \in (0,1)$, we assume that all limit points of the marginals of μ_N at site $[\xi N]$ (where $[x]$ denotes the integer part of x) inherit, as $N \to \infty$, the structure common to $\mu^{T,\varrho}$.

We observe that (i)–(iii) alone are inadequate for determining the sought-after profiles, for they give no information on which T and ϱ are relevant at any given site. The main point of this program is that (a) and (b) *together* is sufficient for uniquely determining the profiles in question.

Remark 2.2 Our rationale for (iii) is as follows: Fix an integer, ℓ. As $N \to \infty$, the gradients of temperature and injection rate on the ℓ sites centered at $[\xi N]$ tend to 0, so that the subsystem consisting of these ℓ sites resembles more and more the situation in (ii). Though rather natural from the point of view of physics [4], this argument does not constitute a proof. Indeed our program is in the direction of proving the existence of well defined Gibbs measures and then assuming, when the system is taken out of equilibrium, that thermodynamic equilibrium is attained locally; in particular, local temperatures are well defined. The full force of local thermal equilibrium is not needed for our purposes; however. The assumption in (iii) pertains only to marginals at single sites.

The rest of this paper is devoted to illustrating the program outlined above in concrete examples.

3 Stochastic Models

3.1 The "random-halves" model

This is perhaps the simplest stochastic model of the general type described in Sect. 2.1. The microscopic laws that govern the dynamics in each cell are as follows: Let $\delta > 0$ be a fixed number. Each tracer is equipped with two independent exponential clocks. Clock 1, which signals the times of energy exchanges with the tanks, rings at rate $\frac{1}{\delta}\sqrt{x}$ where x is the (current) energy of the tracer. Clock 2, which signals the times of site-to-site movements, rings at rate $\sqrt{x}$. The stored energy at site i is denoted by y_i. In the description below, we assume the tracer is at site i.

(i) When Clock 1 rings, the energy carried by the tracer and the stored energy at site i are pooled together and split randomly. That is to say, the tracer gets $p(x + y_i)$ units of energy and the tank gets $(1-p)(x+y_i)$, where $p \in [0, 1]$ is uniformly distributed and independent of all other random variables.

(ii) When Clock 2 rings, the tracer leaves site i. It jumps with equal probability to sites $i \pm 1$. If $i = 1$ or N, going to sites 0 or $N + 1$ means the tracer exits the system.

It remains to specify the coupling to the heat baths. Here it is natural to assume that the energies of the emitted tracers are exponentially distributed with means T_{L} and T_{R}.

This completes the formal description of the model.

Remark 3.1 The rates of the two clocks are to be understood as follows: We assume the energy carried by the tracer is purely kinetic, so that its speed is $\sqrt{x}$. We assume also that a tracer travels, on average, a distance δ between successive interactions with the tank, and a distance 1 before exiting each site.

Remark 3.2 As we will show, the invariant measure does not depend on the value of δ, which can be large or small. The size of δ does affect the rate of convergence to equilibrium, however.

Remark 3.3 While the tracers do not "see" each other in the sense that there is no direct interaction, their evolutions cannot be decoupled. The number of tracers present at a site varies with time. When two or more tracers are present, they interact with the tank whenever their clocks go off, thereby sharing information about their energies. A new tracer may enter at some random moment, bringing its energy to the pool; just as randomly, a tracer leaves, taking with it the energy it happens to be carrying at that time.

3.2 Single-cell analysis

3.2.1 Single cell in equilibrium with 2 identical heat baths

We consider first the following special case of the model described in Sect. 3.1: $N = 1, T_{\mathrm{L}} = T_{\mathrm{R}} = T$, and $\varrho_{\mathrm{L}} = \varrho_{\mathrm{R}} = \varrho$. Each state of the cell in this model is represented by a point in

$$\Omega \;=\; \bigcup_{k=0}^{\infty} \Omega_k \qquad \text{(disjoint union)}$$

where $\Omega_k = \{(\{x_1, \ldots, x_k\}, y) : x_\ell, y \in [0, \infty)\}$. Here $\{x_1, \ldots x_k\}$ is an *unordered* k-tuple representing the energies of the k tracers, y denotes the stored energy, and a point in Ω_k represents a state of the cell when exactly k tracers are present.

Remark 3.4 We motivate our choice of Ω. During a time interval when there are exactly k tracers in the cell – with no tracers entering or exiting – it makes little difference whether we think of the tracers as *named*, and represent the state of the cell by a point in $[0,\infty)^{k+1}$, or if we think of them as *indistinguishable*, and represent the state by a point in Ω_k. With tracers entering and exiting, however, thinking of tracers as named will require that all exiting tracers return later, otherwise the system is transient and has no invariant measure. Since any rule that assigns to each departing tracer a new tracer to carry its name is necessarily artificial, and for present purposes exact identities of tracers play no role, we have opted to regard the tracers as indistinguishable.

We clarify the relationship between $[0,\infty)^{k+1}$ and Ω_k and set some notation: Let $\pi_k : [0,\infty)^{k+1} \to \Omega_k$ be the map $\pi_k(x_1,\dots,x_k,y) = (\{x_1,\dots x_k\},y)$, *i.e.*, π_k is the ($k!$)-to-1 map that forgets the order in the ordered k-tuple $(x_1,\dots,x_k)$. For a measure $\tilde{\mu}$ on $[0,\infty)^{k+1}$ that is symmetric with respect to the x_ℓ coordinates, if $\mu = (\pi_k)_*\tilde{\mu}$, and $\tilde{\sigma}$ and σ are the densities of $\tilde{\mu}$ and μ respectively, then $\tilde{\sigma}$ and σ are related by

$$\sigma(\{x_1,\dots,x_k\},y) \;=\; k!\,\tilde{\sigma}(x_1,\dots,x_k,y)\,.$$

We also write $d\{x_1,\dots,x_k\}dy = (\pi_k)_*(dx_1\dots dx_k dy)$, and use I to denote the characteristic function.

Proposition 3.5 *The model in Sect. 3.1 with $N=1$, $T_{\rm L}=T_{\rm R}=T$, and $\varrho_{\rm L}=\varrho_{\rm R}=\varrho$ has a unique invariant probability measure $\mu=\mu^{T,\varrho}$ on Ω. This measure has the following properties:*

- *the number of tracers present is a Poisson random variable with mean $\varkappa \equiv 2\varrho\sqrt{\pi/T}$, i.e.,*

$$\mu(\Omega_k) \;=\; \frac{\varkappa^k}{k!}e^{-\varkappa}\,, \qquad k=0,1,2,\dots\;; \tag{3.1}$$

- *the conditional density of μ on Ω_k is $c_k\sigma_k d\{x_1,\dots,x_k\}dy$ where*

$$\sigma_k(\{x_1,\dots,x_k\},y) \;=\; I_{\{x_1,\dots,x_k,y\ge 0\}}\,\frac{1}{\sqrt{x_1\cdot\ldots\cdot x_k}}\,e^{-\beta(x_1+\cdots+x_k+y)}\,; \tag{3.2}$$

here $\beta=1/T$, and $c_k=\beta\,k!\,(\beta/\pi)^{k/2}$ is the normalizing constant.

Proof: Uniqueness is straightforward, since one can go from a neighborhood of any point in Ω to a neighborhood of any other point via positive measure sets of sample paths. We focus on checking the invariance of μ as defined above.

For $z,z'\in\Omega$, let $P^h(dz'|z)$ denote the transition probabilities for time $h\ge 0$ starting from z. We fix a small cube $A\subset\Omega_{\bar{k}}$ for some $\bar{k}$, and seek to prove that

$$\frac{d}{dh}\int\left(\int I_A(z')P^h(dz'|z)\right)\mu(dz)\bigg|_{h=0} \;=\; 0\,.$$

On the time interval $(0,h)$, the following three types of events may occur:

Event E_1: Entrance of a new tracer

Event E_2: Exit of a tracer from the cell

Event E_3: Exchange of energy between a tracer and the tank

We claim that with initial distribution μ, the probability of more than one of these events occurring before time h is $o(h)$ as $h \to 0$. This assertion applies to events both of the same type and of distinct types. It follows primarily from the fact that the these events are independent and occur at exponential rates. Of relevance also are the exponential tails of σ_k and the Poisson distribution of $p_k := \mu(\Omega_k)$ in the definition of μ. To illustrate the arguments involved, we will verify at the end of the proof that the probability of two or more tracers exiting on the time interval $(0, h)$ is $o(h)$, but let us accept the above assertion for now and go on with the main argument.

Starting from the initial distribution μ, we let $\mathbf{P}(E_i, A)$ denote the probability that E_i occurs before time h resulting in a state in A, and let $\mathbf{P}(E_1^c \cap E_2^c \cap E_3^c, A)$ denote the probability of starting from a state in A and having none of the E_i occur before time h. We will prove

$$\mathbf{P}(E_1, A) + \mathbf{P}(E_2, A) + \mathbf{P}(E_3, A) + \mathbf{P}(E_1^c \cap E_2^c \cap E_3^c, A) - \mu(A) = o(h)\mu(A) \,. \tag{3.3}$$

Notice that A can be represented as the union of disjoint sets $\cup_i A_i$ where each A_i is of the form

$$A_\varepsilon(\bar{z}) = \{(\{x_1, \ldots, x_{\bar{k}}\}, y) : x_\ell \in [\bar{x}_\ell, \bar{x}_\ell + \varepsilon], \ell = 1, \ldots, \bar{k}, y \in [\bar{y}, \bar{y} + \varepsilon]\}$$

for some $\bar{z} = (\{\bar{x}_1, \ldots, \bar{x}_{\bar{k}}\}, \bar{y}) \in \Omega$, $\varepsilon \ll 1$, and with the intervals $[\bar{x}_\ell, \bar{x}_\ell + \varepsilon]$ pairwise disjoint for $\ell = 1, 2, \ldots, \bar{k}$. To prove (3.3) for A, it suffices to prove it for each A_i provided $o(h)$ in (3.3) is uniformly small for all i.

We consider from here on $A = A_\varepsilon(\bar{z})$ with the properties above. Let σ denote the density of μ. With ε sufficiently small, we have $\mu(A) \approx \sigma(\bar{z})\varepsilon^{\bar{k}+1} = p_{\bar{k}} c_{\bar{k}} \sigma_{\bar{k}}(\bar{z})\varepsilon^{\bar{k}+1}$ where c_k and σ_k are as in the proposition. The other terms in (3.3) are estimated as follows:

$\mathbf{P}(E_1, A)$: E_1 is in fact the union of $2\bar{k}$ subevents, corresponding to a new tracer coming from the left or right bath and the $\bar{k}$ approximate values of energy of the new tracer. For definiteness, we assume the new tracer arrives from the left bath, and has energy in $[\bar{x}_1, \bar{x}_1 + \varepsilon]$. That is to say, the initial state of the cell is described by

$$B = \{(\{x_2, \ldots, x_{\bar{k}}\}, y) : x_\ell \in [\bar{x}_\ell, \bar{x}_\ell + \varepsilon], y \in [\bar{y}, \bar{y} + \varepsilon]\} \ \subset\ \Omega_{\bar{k}-1} \,.$$

The contribution to $\mathbf{P}(E_1, A)$ of this subevent is

$$\begin{aligned} \mu(B)\, h\varrho \int_{\bar{x}_1}^{\bar{x}_1+\varepsilon} \beta e^{-\beta x} dx \quad &\approx \quad h\varrho\, \mu(B)\, e^{-\beta \bar{x}_1}\, \beta\varepsilon \\ &\approx \quad h\varrho\, p_{\bar{k}-1} c_{\bar{k}-1}\, \sigma_{\bar{k}}(\bar{z})\, \sqrt{\bar{x}_1}\, \beta\varepsilon^{\bar{k}+1} \,. \end{aligned}$$

Here, $h\varrho$ is the probability that a tracer is injected, and the integral above is the probability that the injected tracer lies in the specified range. Summing over all $2\bar{k}$ subevents, we obtain

$$\mathbf{P}(E_1, A) \ \approx\ 2h\varrho\beta\, (\sum_{\ell=1}^{\bar{k}} \sqrt{\bar{x}_\ell})\, p_{\bar{k}-1} c_{\bar{k}-1}\, \sigma_{\bar{k}}(\bar{z})\, \varepsilon^{\bar{k}+1} \,. \tag{3.4}$$

$\mathbf{P}(E_2, A)$: In order to result in a state in A, the initial state must be in

$$C_1 = \{(\{x_1, \ldots, x_{\bar{k}}, x\}, y) : x_\ell \in [\bar{x}_\ell, \bar{x}_\ell + \varepsilon], x \in [0, \infty), y \in [\bar{y}, \bar{y} + \varepsilon]\} \ \subset\ \Omega_{\bar{k}+1} \,.$$

We assume here that the tracer with energy x exits between time 0 and time h. This gives

$$\begin{aligned}\mathbf{P}(E_2, A) &\approx p_{\bar{k}+1}\, c_{\bar{k}+1}\, \sigma_{\bar{k}}(\bar{z})\, \varepsilon^{\bar{k}+1} \int_0^\infty \min\{h\sqrt{x}, 1\}\, \frac{1}{\sqrt{x}} e^{-\beta x}\, dx \\ &= p_{\bar{k}+1}\, c_{\bar{k}+1}\, \sigma_{\bar{k}}(\bar{z})\, \varepsilon^{\bar{k}+1}\, \beta^{-1}(h + o(h))\,. \end{aligned} \tag{3.5}$$

$\mathbf{P}(E_3, A)$: For definiteness, we assume it is the tracer with energy near $\bar{x}_1$ that is the product of the interaction with the tank. To arrive in a state in A_ε, one must start from

$$D = \{(\{x_1, \ldots, x_{\bar{k}}\}, y) : x_\ell \in [\bar{x}_\ell, \bar{x}_\ell + \varepsilon] \text{ for } \ell \geq 2, x_1 + y \in [\bar{x}_1 + \bar{y}, \bar{x}_1 + \bar{y} + 2\varepsilon]\}\,.$$

A simple integration using the rule of interaction in Sect. 3.1 gives

$$\mathbf{P}(E_3, A) \approx h\frac{\sqrt{\bar{x}_1}}{\delta}\, p_{\bar{k}} c_{\bar{k}} \sigma_{\bar{k}}(\bar{z}) \varepsilon^{\bar{k}+1}\,. \tag{3.6}$$

$\mathbf{P}(E_1^c \cap E_2^c \cap E_3^c, A)$: We first note that starting from A, the probability of the tracer with energy $\approx \bar{x}_1$ exiting is

$$p_{\bar{k}} c_{\bar{k}} \sigma_{\bar{k}}(\bar{z}) \sqrt{\bar{x}_1} e^{\beta \bar{x}_1} \varepsilon^{\bar{k}} \int_{\bar{x}_1}^{\bar{x}_1+\varepsilon} h\sqrt{x} \frac{1}{\sqrt{x}} e^{-\beta x} dx \;=\; h\sqrt{\bar{x}_1}\, p_{\bar{k}} c_{\bar{k}} \sigma_{\bar{k}}(\bar{z})\, \varepsilon^{\bar{k}+1}\,;$$

the probability of the tracer with energy $\approx \bar{x}_1$ interacting with the tank is

$$h\frac{\sqrt{\bar{x}_1}}{\delta}\, p_{\bar{k}} c_{\bar{k}} \sigma_{\bar{k}}(\bar{z})\, \varepsilon^{\bar{k}+1}\,;$$

and the probability of a new tracer entering the cell from the left (resp. right) bath is $h\varrho\, \mu(A_\varepsilon)$. Thus

$$\begin{aligned}\mathbf{P}(E_1^c \cap E_2^c \cap E_3^c, A) &\approx p_{\bar{k}} c_{\bar{k}} \sigma_{\bar{k}}(\bar{z})\, \varepsilon^{\bar{k}+1} \cdot \Pi_\ell(1 - h\sqrt{\bar{x}_\ell}) \cdot (1 - h\varrho)^2 \cdot \Pi_\ell(1 - h\sqrt{\bar{x}_\ell}/\delta) \\ &\approx p_{\bar{k}} c_{\bar{k}} \sigma_{\bar{k}}(\bar{z})\, \varepsilon^{\bar{k}+1} \cdot \left(1 - h\left(\Sigma_{\ell=1}^{\bar{k}} \sqrt{\bar{x}_\ell} + 2\varrho + \frac{1}{\delta} \Sigma_{\ell=1}^{\bar{k}} \sqrt{\bar{x}_\ell}\right)\right). \end{aligned} \tag{3.7}$$

Summing Eqs. (3.4)–(3.7), we obtain (3.3) provided

$$2\varrho\beta p_{\bar{k}-1} c_{\bar{k}-1} \;=\; p_{\bar{k}} c_{\bar{k}} \qquad \text{and} \qquad 2\varrho p_{\bar{k}} c_{\bar{k}} \;=\; p_{\bar{k}+1} c_{\bar{k}+1} T\,.$$

Note that these two equations represent the same relation for different k. We write this relation as

$$\frac{c_k p_k}{c_{k+1} p_{k+1}} = \frac{T}{2\varrho}\,, \tag{3.8}$$

and verify that it is compatible with assertion (3.1): Since

$$c_k\, \frac{1}{k!} \left(\Pi_{\ell=1}^k \int \frac{1}{\sqrt{x_\ell}} e^{-\beta x_\ell} dx_\ell\right) \int e^{-\beta y} dy \;=\; 1\,,$$

and $\int_0^\infty x^{-1/2} e^{-\beta x} dx = \sqrt{\pi T}$, we have

$$p_{k+1} \;=\; \frac{2\varrho}{T}\, \frac{c_k}{c_{k+1}}\, p_k \;=\; \frac{2\varrho}{T} \left(\frac{1}{k+1} \int_0^\infty \frac{1}{\sqrt{x}} e^{-\beta x} dx\right) p_k \;=\; \frac{1}{k+1}\, \frac{2\sqrt{\pi}\varrho}{\sqrt{T}}\, p_k\,.$$

To complete the proof, we estimate the probability of two or more tracers exiting before time h. For $n = 2, 3, \ldots$, let $E_{2,n}$ be the event that the initial state is in

$$C_n = \{(\{x_1, \ldots, x_{\bar{k}}, x^{(1)}, \ldots, x^{(n)}\}, y) : x_\ell \in [\bar{x}_\ell, \bar{x}_\ell + \varepsilon], x^{(\ell')} \in [0, \infty), y \in [\bar{y}, \bar{y} + \varepsilon]\} \ ,$$

and during the time interval $(0, h)$, all n of the tracers carrying energies $x^{(\ell')}$, $\ell' = 1, 2, \ldots, n$, exit the system. The probability of $\cup_{n \geq 2} E_{2,n}$ is

$$\sum_{n \geq 2} p_{\bar{k}+n} c_{\bar{k}+n} \sigma_{\bar{k}}(\bar{z}) \varepsilon^{\bar{k}+1} \left(\mathcal{O}(h)\right)^n \ ,$$

which, from Eq. (3.8), is bounded by

$$p_{\bar{k}} c_{\bar{k}} \sigma_{\bar{k}}(\bar{z}) \varepsilon^{\bar{k}+1} \sum_{n \geq 2} \left(\frac{2\varrho}{T}\right)^n \left(\mathcal{O}(h)\right)^n \ = \ p_{\bar{k}} c_{\bar{k}} \sigma_{\bar{k}}(\bar{z}) \varepsilon^{\bar{k}+1} \ o(h) \ .$$

$\square$

Remark 3.6 In the setting of Proposition 3.5, since the cell is in equilibrium with the two heat baths, it is obvious that it ejects, on average, 2ϱ tracers per unit time, and the energies of the tracers ejected have mean T. We observe that the cell in fact reciprocates the action of the bath more strongly than this: the *distribution* of the energies of the ejected tracers is also exponential. To see this, fix k and consider one tracer at a time. The probability of the tracer exiting with energy $> u$ is

$$\sim \int_u^\infty \sqrt{x} \cdot \frac{1}{\sqrt{x}} e^{-\beta x} dx \ = \ \beta^{-1} e^{-\beta u} \ .$$

3.2.2 Chain of N cells in equilibrium with 2 identical heat baths

We treat next the case of arbitrary N. That is to say, the system is as defined in Sect. 3.1, but with $T_{\rm L} = T_{\rm R} = T$ and $\varrho_{\rm L} = \varrho_{\rm R} = \varrho$. Let μ be as in Proposition 3.5.

Proposition 3.7 *The N-fold product $\mu \times \cdots \times \mu$ is invariant.*

Remark 3.8 That the invariant measure is a product tells us that at steady state, there are no spatial correlations. We do not find this to be entirely obvious on the intuitive level: one might think that above-average energy levels on the left half of the chain may cause the right half to be below average; that is evidently not the case. This result should not be confused with the absence of *space-time* correlations.

Proof: Proceeding as before, we consider a small time interval $(0, h)$, and treat separately the individual events that may occur during this period. One of the new events (not relevant in the case of a single cell) is the jumping of a tracer from site $i \pm 1$ to site i. We fix a phase point

$$\bar{z} \ = \ (\bar{z}^{(1)}, \ldots, \bar{z}^{(N)}) \ = \ (\{\bar{x}_1^{(1)}, \ldots, \bar{x}_{k_1}^{(1)}\}, y^{(1)}; \ \ldots; \ \{\bar{x}_1^{(N)}, \ldots, \bar{x}_{k_N}^{(N)}\}, y^{(N)}) \ ,$$

and let $A = \Pi_{i=1}^N A^{(i)} \subset \Omega^N$ where $A^{(i)} = A_\varepsilon(\bar{z}^{(i)})$ is as in Proposition 3.5. Let $\sigma^{(i)} = \sigma_{k_i}(\bar{z}^{(i)})$. For definiteness, we fix also an integer $n, 1 < n < N$, and assume that at time 0, the state of the chain is as follows:

(i) at site $n+1$, there are $k_{n+1}+1$ tracers the energies of which lie in disjoint intervals

$$[\bar{x}_1^{(n+1)}, \bar{x}_1^{(n+1)}+\varepsilon], \ \ldots, \ [\bar{x}_{k_{n+1}}^{(n+1)}, \bar{x}_{k_{n+1}}^{(n+1)}+\varepsilon] \quad \text{and} \quad [\bar{x}_1^{(n)}, \bar{x}_1^{(n)}+\varepsilon] \ ,$$

(ii) at site n, there are $k_n - 1$ tracers whose energies lie in

$$[\bar{x}_2^{(n)}, \bar{x}_2^{(n)}+\varepsilon], \ \ldots, \ [\bar{x}_{k_n}^{(n)}, \bar{x}_{k_n}^{(n)}+\varepsilon] \ .$$

The probability of this event occurring *and* the tracer with energy $\approx \bar{x}_1^{(n)}$ jumping from site $n+1$ into site n is then given by $\frac{1}{2} I \cdot \mathit{II} \cdot \mathit{III}$ where

$$\begin{aligned}
I &= \Pi_{i\neq n,n+1} \, (p_{k_i} c_{k_i} \sigma^{(i)} \varepsilon^{k_i+1}) \\
\mathit{II} &= p_{k_n-1} c_{k_n-1} \sigma^{(n)} \sqrt{\bar{x}_1^{(n)}} e^{\beta \bar{x}_1^{(n)}} \varepsilon^{k_n} \\
\mathit{III} &= p_{k_{n+1}+1} c_{k_{n+1}+1} \sigma^{(n+1)} \varepsilon^{k_{n+1}+1} \ \int_{\bar{x}_1^{(n)}}^{\bar{x}_1^{(n)}+\varepsilon} h\sqrt{x} \frac{1}{\sqrt{x}} e^{-\beta x} dx \ .
\end{aligned}$$

This product can be written as

$$\frac{h}{2} \left(\Pi_{i=1}^N p_{k_i} c_{k_i} \sigma^{(i)} \varepsilon^{k_i+1} \right) \cdot \frac{p_{k_n-1}}{p_{k_n}} \frac{c_{k_n-1}}{c_{k_n}} \cdot \frac{p_{k_{n+1}+1}}{p_{k_{n+1}}} \frac{c_{k_{n+1}+1}}{c_{k_{n+1}}} \cdot \sqrt{\bar{x}_1^{(n)}} \ ,$$

which, by Eq. (3.8), is equal to

$$\frac{h}{2} \left(\Pi_{i=1}^N p_{k_i} c_{k_i} \sigma^{(i)} \varepsilon^{k_i+1} \right) \cdot \sqrt{\bar{x}_1^{(n)}} \ . \tag{3.9}$$

There are many terms of this kind that contribute to $\int I_A(z') P^h(dz'|z) \mu(dz)$, two for $\bar{x}_\ell^{(n)}$ for each pair (n, ℓ). We claim that the system has detailed balance, *i.e.*, the term associated with the scenario above is balanced by the probability of starting from a state in A and having the tracer at site n carrying energy $\approx \bar{x}_1^{(n)}$ jump to site $n+1$. The probability of the latter is

$$\frac{1}{2} (\Pi_{i=1}^N p_{k_i} c_{k_i} \sigma^{(i)} \varepsilon^{k_i+1}) \cdot \sqrt{\bar{x}_1^{(n)}} e^{\beta \bar{x}_1^{(n)}} \frac{1}{\varepsilon} \cdot \int_{\bar{x}_1^{(n)}}^{\bar{x}_1^{(n)}+\varepsilon} h\sqrt{x} \frac{1}{\sqrt{x}} e^{-\beta x} dx \ ,$$

which balances exactly (3.9) as claimed.

An argument combining the one above with that in Proposition 3.5 regarding the injection of new tracers holds at sites 1 and N. □

Propositions 3.5 and 3.7 are steps (i) and (ii) in the proposed scheme in Sect. 2.2.

3.3 Derivation of equations of macroscopic profiles

Having found a candidate family of equilibrium measures $\{\mu^{T,\varrho}\}$, we now complete the rest of the program outlined in Sect. 2.2. The next step, according to this program, is to *assume* that for $N \gg 1$, the marginals of the invariant measure μ_N at site i are approximately equal to $\mu^{T,\varrho}$ for some $T = T_i$ and $\varrho = \varrho_i$. We identify those parts of our proposed theory that are not proved in this paper and state them precisely as "Assumptions".

Assumption 1. *Given $T_\mathrm{L}, T_\mathrm{R} > 0$, $\varrho_\mathrm{L}, \varrho_\mathrm{R} \geq 0$, and $N \in \mathbb{Z}^+$, the N-chain defined in Sect. 3.1 with these parameters has an invariant probability measure μ_N.*

We do not believe this existence result is hard to prove but prefer not to depart from the main line of reasoning in this paper. Once existence is established, uniqueness (or ergodicity) follows easily since any invariant measure clearly has strictly positive density everywhere. A proof of the statement in Assumption 2 below is more challenging. For $\xi \in (0,1)$, let $\mu_{N,[\xi N]}$ denote the marginal of μ_N at the site $[\xi N]$.

Assumption 2. *For every $\xi \in (0,1)$, every limit point as $N \to \infty$ of $\mu_{N,[\xi N]}$ is a member of the family $\{\mu^{T,\varrho},\ T > 0, \varrho \geq 0\}$.*[1]

In Sect. 2.1, we introduced four quantities of interest. There is one that was somewhat ambiguously defined, namely e_i. Its precise meaning is as follows: $e_i := \sum_{k=1}^{\infty} p_{i,k} e_{i,k}$ where $p_{i,k}$ is the probability that the number of tracers at site i is equal to k and $e_{i,k}$ is $\frac{1}{k}$ of the mean total tracer energy conditioned on the number of tracers present being equal to k.

Theorem 3.9 is about the profiles of certain observables as $N \to \infty$. We refer the reader to the end of Sect. 2.1 for the precise meaning of the word "profile" in the theorem.

Theorem 3.9 *The following hold for the "random-halves" model defined in Sect. 3.1 with arbitrary $T_\mathrm{L}, T_\mathrm{R}, \varrho_\mathrm{L}, \varrho_\mathrm{R}$. Under Assumptions 1 and 2 above:*

- *the profile for the mean number of jumps out of a site per unit time is*

$$j(\xi) \;=\; 2(\varrho_\mathrm{L} + (\varrho_\mathrm{R} - \varrho_\mathrm{L})\xi) \;.$$

- *the profile for the mean total energy transported out of a site per unit time is*

$$Q(\xi) \;=\; 2(\varrho_\mathrm{L} T_\mathrm{L} + (\varrho_\mathrm{R} T_\mathrm{R} - \varrho_\mathrm{L} T_\mathrm{L})\xi) \;;$$

- *the profile for the mean stored energy at a site is*

$$s(\xi) \;=\; \frac{Q(\xi)}{j(\xi)} \;=\; \frac{\varrho_\mathrm{L} T_\mathrm{L} + (\varrho_\mathrm{R} T_\mathrm{R} - \varrho_\mathrm{L} T_\mathrm{L})\xi}{\varrho_\mathrm{L} + (\varrho_\mathrm{R} - \varrho_\mathrm{L})\xi} \;;$$

  in the case $\varrho_\mathrm{L} = \varrho_\mathrm{R}$, this simplifies to $s(\xi) = T_\mathrm{L} + (T_\mathrm{R} - T_\mathrm{L})\xi$;
- *the profile for mean tracer energy is $e(\xi) = \frac{1}{2} s(\xi)$;*
- *the profile for mean number of tracers is*

$$\varkappa(\xi) \;=\; \sqrt{\frac{\pi}{s(\xi)}}\, j(\xi) \;;$$

- *the profile for mean total-cell energy is*

$$E(\xi) \;=\; s(\xi) + \varkappa(\xi) e(\xi) \;=\; s(\xi) + \frac{1}{2}\sqrt{\pi s(\xi)}\, j(\xi) \;.$$

[1] As stated in Section 2, we assume all marginals $\mu_{N,[\xi N]}$, $N \geq 1$, have uniform tail bounds in energy and in number of tracers of the type suggested in the single-cell analysis.

Proof of Theorem 3.9 : We divide the proof into the following three steps:

I. Information on single cells: Items (i)–(iv) are strictly in the domain of *internal cell dynamics*. The setting is that of Proposition 3.5, and the results below are deduced (in straightforward computations) from the invariant density given by that proposition. The parameters are, as usual, T and ϱ. (Note that this means the rate at which tracers enter the site is 2ϱ.)

(i) stored energy has density $\beta e^{-\beta y}$ and mean T ;
(ii) tracer energy has density $\frac{\sqrt{\beta}}{\sqrt{\pi x}} e^{-\beta x}$ and mean $\frac{T}{2}$;
(iii) mean number of tracers, $\varkappa = 2\sqrt{\frac{\pi}{T}}\varrho$;
(iv) mean total-cell energy, $E = T \cdot (1 + \frac{\varkappa}{2})$.

Items (v) and (vi) are in preparation for the analysis of *cell-to-cell traffic* :

(v) mean number of jumps out of the cell per unit time, $j = 2\varrho$;
(vi) mean total energy transported out of the cell per unit time, $Q = Tj$.

II. Global phenomenological equations: Consider now a chain with N cells with settings $T_{\rm L}, T_{\rm R}, \varrho_{\rm L}$ and $\varrho_{\rm R}$ at the two ends. The following results use only standard conservation laws together with the local rule that when a tracer exits a cell, it has equal probability of going left and right.

(A) *Balancing tracer fluxes:* Let j_i denote the number of jumps per unit time out of site i. Then

$$j_i = 2\left(\varrho_{\rm L} + \frac{i}{N+1}(\varrho_{\rm R} - \varrho_{\rm L})\right) . \tag{3.10}$$

Proof: Consider an (imaginary) partition between site i and site $i+1$. We let $-\Delta j_i$ denote the flux across this partition. Then $\Delta j_i = \frac{1}{2}(j_{i+1} - j_i)$ for $i = 0, 1, \ldots, N$ where j_0 and j_{N+1} are defined to be $2\varrho_{\rm L}$ and $2\varrho_{\rm R}$ respectively. For $i \neq 0, N$, the $\frac{1}{2}$ is there because only half of the tracers out of site $i+1$ jump left, and half of those out of site i jump right. The fluxes across partitions between all consecutive sites must be equal, or there would be a pile-up of tracers somewhere. This together with $\sum_i \Delta j_i = 2(\varrho_{\rm R} - \varrho_{\rm L})$ gives the asserted formula.

(B) *Balancing energy fluxes:* Let Q_i denote the mean total energy transported out of site i per unit time. Then

$$Q_i = 2\left(\varrho_{\rm L} T_{\rm L} + \frac{i}{N+1}(\varrho_{\rm R} T_{\rm R} - \varrho_{\rm L} T_{\rm L})\right) .$$

Proof: The argument is identical to that in (A), with $\Delta Q_i = \frac{1}{2}(Q_{i+1} - Q_i)$ and Q_0 and Q_{N+1} defined to be $2\varrho_{\rm L} T_{\rm L}$ and $2\varrho_{\rm R} T_{\rm R}$ respectively.

III. Combining the results from I and II: Fix $\xi \in (0, 1)$. Passing to a subsequence if necessary, we have, by Assumption 2, $\mu_{N,[\xi N]} \to \mu^{T(\xi),\varrho(\xi)}$ for some $T(\xi)$ and $\varrho(\xi)$. We identify the two numbers $T(\xi)$ and $\varrho(\xi)$ as follows:

Let $j^N(\xi)$ denote the mean number of jumps out of site $[\xi N]$ per unit time in the N-chain. Then by (A) in part II, $j(\xi) := \lim_{N\to\infty} j^N(\xi) = 2(\varrho_{\rm L} + (\varrho_{\rm R} - \varrho_{\rm L})\xi)$. This is, therefore, the mean number of jumps out of a cell with invariant measure $\mu^{T(\xi),\varrho(\xi)}$. Similarly, we deduce that the mean total energy transported out of a cell with the same invariant measure is $Q(\xi) := \lim_{N\to\infty} Q^N(\xi) =$

$2(\varrho_L T_L + (\varrho_R T_R - \varrho_L T_L)\xi)$. Appealing now to the information in part I, we deduce from (v) and (vi) that $\varrho(\xi) = \frac{1}{2}j(\xi)$ and $T(\xi) = Q(\xi)/j(\xi)$.

The rest of the profiles follow readily: we read off $s = T$ from (i), and deduce the relation between s and e by comparing (i) and (ii). The profiles for $\varkappa$ and E follow from (iii) and (iv) together with our knowledge of ϱ and T. The proof of Theorem 3.9 is complete. □

We remark that in the terminology of [7] our random halves model is of *gradient type*.

Remark 3.10 It is instructive to see what Theorem 3.9 says in the special case when $\varrho_L = 0$. Since no particles are injected at the left end, clearly, T_L cannot matter. But since tracers do exit from the left, one expects an energy flux across the system. Upon substituting $\varrho_L = 0$ into the formulas above, one gets

$$j(\xi) = 2\varrho_R \xi \ , \quad e(\xi) = \tfrac{1}{2}s(\xi) = \tfrac{1}{2}T_R \ , \quad \varkappa(\xi) = 2\varrho_R \xi \sqrt{\pi/T_R} \ ,$$

and an energy flux of $-\frac{1}{2}Q'(\xi) = -\varrho_R T_R$.

3.4 Simulations

Numerical simulations are used to validate Assumptions 1 and 2 in Theorem 3.9 .

We mention here only those details of the simulations that differ from the theoretical study. Needless to say, we work with a finite number of sites, usually 20. Simulations start in a random initial state, and are first run for a period of time to let the system reach its steady state. All times are in number of events (E_1, E_2, and E_3). Up to half the simulation time is used to reach stationarity; statistics are then gathered during the remaining simulation time. Since total simulation time is finite, we find it necessary to take measures to deal with tracers of exceptionally low energy: these tracers appear to remain in a cell indefinitely, skewing the statistics on the number of tracers. We opted to terminate events involving a single tracer at a single site after about 0.001 of total simulation time. This was done about 10 times in the course of 10^9 events.

Simulations are performed both to verify directly the properties of the marginals at individual sites and to plot empirically the various profiles of interest. Excellent agreement with predicted values is observed in all runs. A sample of the results is shown in Fig. 1.

3.5 Interpretation of results

We gather here our main observations, discuss their physical implications, and provide explanations for the reasons behind the derived formulas.

1. Linearity of profiles

We distinguish between the following 3 types of profiles:

a. *Transport of energy and tracers*: $j(\xi)$ and $Q(\xi)$ are always linear by simple conservation laws and by the imposed left-right symmetry in outflow of tracers and energy from each site.

b. *Mean stored and (individual) tracer energies*: $s(\xi)$ and $e(\xi)$ are linear if and only if there is no tracer flux across the system. (See item 4 below.)

c. *Tracer densities and total-cell energy*: $\varkappa(\xi)$ is never linear (unless $T_L = T_R$ and $\varrho_L = \varrho_R$); in addition to the obvious bias brought about by different injection rates, tracers have a tendency to accumulate at the cold end (see item 3 for elaboration). As a result, $E(\xi)$ is also never linear.

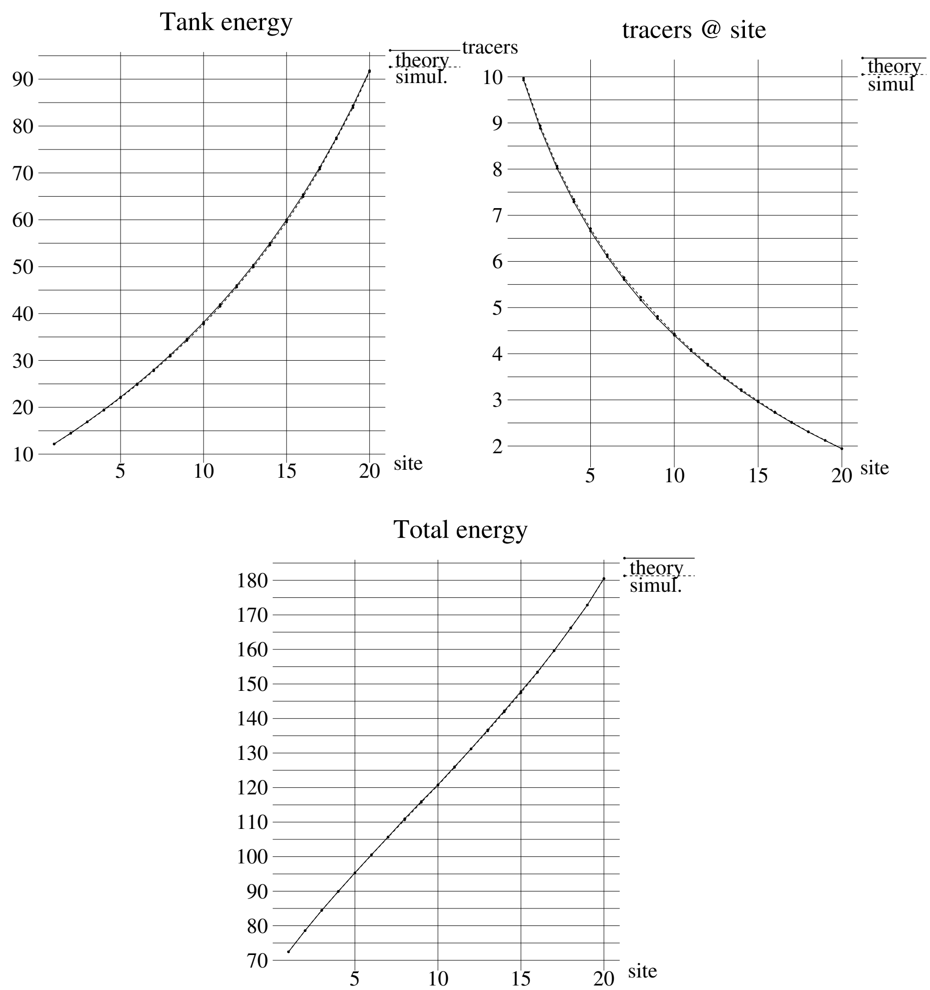

Figure 1: Random-halves model with 20 sites, temperatures $T_{\mathrm{L}} = 10$, $T_{\mathrm{R}} = 100$ and injection rates $\varrho_{\mathrm{L}} = 10$, $\varrho_{\mathrm{R}} = 5$. Top left: Mean tank energies s_i. Top right: Mean number of tracers $\varkappa_i$. Bottom: Mean total energy E_i. Simulations in perfect agreement with predictions from theory.

2. Heat flux and the Fourier Law

Heat flux from left to right is given by $\Phi = T_{\rm L}\varrho_{\rm L} - T_{\rm R}\varrho_{\rm R}$. Thinking of the temperature of the system as given by $T(\xi)$, Theorem 3.9 says that thermal conductivity is constant and proportional to $T_{\rm R} - T_{\rm L}$ if and only if there is no tracer flux across the system, *i.e.*, if and only if $\varrho_{\rm L} = \varrho_{\rm R}$.

3. Distribution of tracers along the chain

In the case $\varrho_{\rm L} = \varrho_{\rm R}$, more tracers are congregated at the cold end than at the hot. This is because the only way to balance the tracer equation is to have the number of jumps out of a site be constant along the chain. Inside the cells, however, tracers move more slowly at the cold end, hence they jump less frequently, and the only way to maintain the required number of jumps is to have more tracers. When $\varrho_{\rm L} \neq \varrho_{\rm R}$, the idea above continues to be valid, except that one needs also to take into consideration the bias in favor of more tracers at the end where the injection rate is higher.

4. Tracer flux and concavity of stored energy

One of the interesting facts that have emerged is that $s(\xi)$ is linear if and only if $\varrho_{\rm L} = \varrho_{\rm R}$, and when $\varrho_{\rm L} \neq \varrho_{\rm R}$, their relative strength is reflected in the concavity of $s(\xi)$. This may be a little perplexing at first because no mechanism is built into the microscopic rules for the tanks to recognize the directions of travel of the tracers with which they come into contact. The reason behind this phenomenon is, in fact, quite simple: If there is a tracer flux across the system, say from right to left, then the tank at site i hears from site $i+1$ more frequently than it hears from site $i-1$ (because $j_{i+1} > j_{i-1}$). It therefore has a greater tendency to equilibrate with the energy level on the right than on the left, causing s_i to be $> \frac{1}{2}(s_{i+1} + s_{i-1})$. Since this happens at every site, a curvature for the profile of s_i is created. The reader should further note that tracer flux and heat flux go in opposite directions if $(\varrho_{\rm L} - \varrho_{\rm R}) \cdot (\varrho_{\rm L} T_{\rm L} - \varrho_{\rm R} T_{\rm R}) < 0$.

5. Individual cells mimicking heat baths

The cells in our models are clearly not infinite heat reservoirs, yet for large N, they acquire some of the characteristics of the heat baths with which they are in contact. More precisely, the ith cell injects each of its two neighbors with ϱ_i tracers per unit time. These tracers, which have mean energy T_i, are distributed according to a law of the same type as that with which tracers are emitted from the baths (exponential in the case of the random halves model); see Remark 3.6. Unlike the conditions at the two ends, however, the numbers ϱ_i and T_i are *self-selected.*

3.6 A second example

We consider here a model of the same type as the "random-halves" model but with *different microscopic rules*. The purpose of this exercise is to highlight the role played by these rules and to make transparent which part of our scheme is generic.

The rules for energy exchange in this model simulate a Hamiltonian model in which both tracers and tanks have one degree of freedom. Write $x = v^2$ and $y = \omega^2$, $v, \omega \in (-\infty, \infty)$, and think of energy as uniformly distributed on the circle $\{(v, \omega) : v^2 + \omega^2 = c\}$, so that when the tracer interacts with stored energy, the redistribution is such that a random point on this circle is chosen with weight $|v|$ (this is the measure induced on a cross-section by the invariant measure of the flow). That is to say, if (x, y) are the stored energy and tracer energy before an interaction, and (x', y') afterwards, then for $a \in [0, x+y]$,

$$P\{y' > a\} \;=\; P\{|\omega'| > \sqrt{a}\} \;=\; 1 - \frac{\int_0^{\sqrt{a}} v\sqrt{1+\left(\frac{dv}{d\omega}\right)^2}d\omega}{\int_0^{\sqrt{x+y}} v\sqrt{1+\left(\frac{dv}{d\omega}\right)^2}d\omega} \;=\; 1 - \frac{\sqrt{a}}{\sqrt{x+y}} \,, \qquad (3.11)$$

or, equivalently, the density of y' is

$$\frac{1}{2}\frac{1}{\sqrt{y'}}\frac{1}{\sqrt{x+y}} \qquad \text{for} \quad y' \in [0, x+y] \,.$$

Assume now that all is as in Sect. 3.1, except that when Clock 1 of a tracer rings, it exchanges energy with the tank according to the rule in (3.11) and not the random-halves rule. Following the computation in Sect. 3.2 (details of which are left to the reader), we see that Propositions 3.5 and 3.7 hold for the present model provided σ_k is replaced by

$$\sigma_k(\{x_1, \cdot \cdot \cdot \cdot, x_k\}, y) \;=\; I_{\{x_1,\ldots,x_k,y\geq 0\}}\, \frac{1}{\sqrt{x_1 \cdot \ldots \cdot x_k y}}\, e^{-\beta(x_1+\ldots+x_k+y)} \,.$$

This defines a new family of $\{\hat{\mu}^{T,\varrho}\}$ for this model. With $\hat{\mu}^{T,\varrho}$ in hand, we make the assumption as before that for $N \gg 1$, the marginals of individual sites have the same form. Proceeding as in Sect. 3.3, we read off the following information on single cells:

(i) stored energy has density $\text{const.}e^{-\beta y}/\sqrt{y}$ and mean $T/2$;
(ii) tracer energy has density $\text{const.}e^{-\beta x}/\sqrt{x}$ and mean $T/2$;
(iii) mean number of tracers, $\varkappa = 2\sqrt{\frac{\pi}{T}}\varrho$;
(iv) mean total-cell energy, $E = \frac{T}{2}(1+\varkappa)$.

The rest of the analysis, including (iv), (v), (A) and (B), do not depend on the local rules (aside from the fact that tracers exiting a cell have equal chance of going left and right). Thus they remain unchanged. Reasoning as in Theorem 3.9, we obtain the following:

Proposition 3.11 *Under Assumptions 1 and 2, the profiles for the model with energy exchange rule (3.11) are*

- $j(\xi) \;=\; 2(\varrho_{\mathrm{L}} + (\varrho_{\mathrm{R}} - \varrho_{\mathrm{L}})\xi)$;
- $Q(\xi) \;=\; 2(\varrho_{\mathrm{L}}T_{\mathrm{L}} + (\varrho_{\mathrm{R}}T_{\mathrm{R}} - \varrho_{\mathrm{L}}T_{\mathrm{L}})\xi)$;
- $s(\xi) \;=\; e(\xi) \;= \frac{1}{2}\, Q(\xi)/j(\xi)$;
- $\varkappa(\xi) \;=\; \sqrt{2\pi/s(\xi)}\, j(\xi)/2$;
- $E(\xi) \;=\; s(\xi) + \varkappa(\xi)e(\xi) \;=\; s(\xi) + \sqrt{2\pi s(\xi)}\, j(\xi)/2$.

Numerical simulations give results in excellent agreement with these theoretical predictions.

4 Hamiltonian Models

In Sect. 4.1, we introduce a family of Hamiltonian models generalizing those studied numerically in [17, 12]. A single-cell analysis similar to that in Section 3 is carried out for this family in Sect. 4.2, and predictions of energy and tracer density profiles are made in Sect. 4.3. We again use the Assumptions in Section 3, but the predictions here are made under an additional ergodicity assumption, ergodicity being a property that is easy to arrange in stochastic models but not in Hamiltonian ones. Results of simulations for a specific model are shown in Sect. 4.5. A brief discussion of related models is given in Sect. 4.6.

4.1 Rotating disks models

We describe in this subsection a family of models quite close to those studied numerically in [17, 12]. The rules of interaction (though not the coupling to heat baths) are, in fact, used earlier in [20].

4.1.1 Dynamics in a closed cell

We treat first the dynamics within individual cells assuming the cell or box is *sealed*, *i.e.*, it is not connected to its neighbors or to external heat sources.

Let $\Gamma_0 \subset \mathbb{R}^2$ be a bounded domain with piecewise C^3 boundary. In the interior of Γ_0 lies a (circular) disk D, which we think of as nailed down at its center. This disk rotates freely, carrying with it a finite amount of kinetic energy derived from its angular velocity; it will play the role of the "energy tank" in Sect. 2.1. The system below describes the free motion of k point particles (*i.e.*, tracers) in $\Gamma = \Gamma_0 \setminus D$. When a tracer runs into $\partial\Gamma_0$, the boundary of Γ_0, the reflection is specular. When it hits the rotating disk, the energy exchange is according to the rules introduced in [20, 17, 12]. A more precise description of the system follows.

The phase space of this dynamical system is

$$\bar{\Omega}_k = (\Gamma^k \times \partial D \times \mathbb{R}^{2k+1})/\sim$$

where

$\mathbf{x} = (x_1, \ldots, x_k) \in \Gamma^k$ denotes the positions of the k tracers,
$\vartheta \in \partial D$ denotes the angular position of a (marked) point on the boundary of the turning disk,
$\mathbf{v} = (v_1, \ldots, v_k) \in \mathbb{R}^{2k}$ denotes the velocities of the k tracers,
$\omega \in \mathbb{R}$ denotes the angular velocity of the turning disk,

and $\sim$ is a relation that identifies pairs of points in the collision manifold $M_k = \{(\mathbf{x}, \vartheta, \mathbf{v}, \omega) : x_\ell \in \partial\Gamma \text{ for some } \ell\}$. The rule of identification is given below.

The flow on $\bar{\Omega}_k$ is denoted by $\bar{\Phi}_s$. As long as no collisions are involved, we have

$$\bar{\Phi}_s\,(\mathbf{x}, \vartheta, \mathbf{v}, \omega) \;=\; (\mathbf{x} + s\mathbf{v}, \vartheta + s\omega, \mathbf{v}, \omega)\,.$$

We assume at most one tracer collides with $\partial\Gamma$ at any one point in time. ($\bar{\Phi}_s$ is not defined at multiple collisions, which occur on a set of measure zero.) At the point of impact, *i.e.*, when $x_\ell \in \partial\Gamma$ for one of the ℓ, let $v_\ell = (v_\ell^{\mathrm{t}}, v_\ell^{\mathrm{n}})$ be the tangential and normal components of v_ℓ. What happens subsequent to impact depends on whether $x_\ell \in \partial\Gamma_0$ or ∂D. In the case of a collision with $\partial\Gamma_0$, the tracer bounces off $\partial\Gamma_0$ with angle of reflection equal to angle of incidence, *i.e.*,

$$(v_\ell^{\mathrm{n}})' = -v_\ell^{\mathrm{n}}, \qquad (v_\ell^{\mathrm{t}})' = v_\ell^{\mathrm{t}}\;, \tag{4.12}$$

and the other variables are unchanged. In the case of a collision with the disk, the following *energy exchange* takes place between the disk and the tracer:

$$(v_\ell^{\mathrm{n}})' = -v_\ell^{\mathrm{n}}, \qquad (v_\ell^{\mathrm{t}})' = \omega\;, \qquad \omega' = v_\ell^{\mathrm{t}}\;. \tag{4.13}$$

Here we have, for simplicity, taken the radius of the disk, the moment of inertia of the disk, and the mass of tracer in such a way that the coefficients in Eq. (4.13) are equal to 1. The identification in the definition of $\bar{\Omega}_k$ is $z \sim z'$ where $z, z' \in M_k$ are such that all of their coordinates are equal except that v_ℓ and ω in z are replaced by the corresponding quantities with primes in Eqs. (4.12) and (4.13) for z'. We also write $F(z) = z'$.

Note that in both (4.12) and (4.13), total energy is conserved, *i.e.*, $|v|^2 + \omega^2 = |v'|^2 + (\omega')^2$. The energy surfaces in this model are therefore

$$\bar{\Omega}_{k,E} \;=\; (\Gamma^k \times \partial D \times S_E^{2k})/\sim$$

where

$$S_E^{2k} = \{(v_1, \ldots, v_k, \omega) \in \mathbb{R}^{2k+1} : \sum |v_\ell|^2 + \omega^2 = E\}\ .$$

We claim that the natural invariant measure, or Liouville measure, of the (discontinuous) flow $\bar{\Phi}_s$ on $\bar{\Omega}_k$ is

$$\bar{m}_k = (\lambda_2|_\Gamma)^k \times (\nu_1|_{\partial D}) \times \lambda_{2k+1}$$

where λ_d is d-dimensional Lebesgue measure and ν_d is surface area on the relevant d-sphere. Once the invariance of $\bar{m}_k$ is checked, it will follow immediately that the induced measures $\bar{m}_{k,E} = (\lambda_2|_\Gamma)^k \times (\nu_1|_{\partial D}) \times \nu_{2k}$ on $\bar{\Omega}_{k,E}$ are $\bar{\Phi}_s$-invariant, as are all measures on $\bar{\Omega}_k$ of the form $\psi(E)\bar{m}_{k,E}$ for some $\psi : [0, \infty) \to [0, \infty)$.

The invariance of $\bar{m}_k$ is obvious away from collisions and at collisions with $\partial\Gamma_0$. Because collisions occur one at a time, it suffices to consider a single collision between a single tracer and the disk. The problem, therefore, is reduced to the following: Consider $\bar{\Phi}_s$ on $\bar{\Omega}_1$, and let $M_{1,D}$ denote the part of the collision manifold involving D. To prove that $\bar{m}_1$ is preserved in a collision with D, if suffices to check that for $A \subset M_{1,D}$ and $\varepsilon > 0$ arbitrarily small,

$$\bar{m}_1(\,\cup_{-\varepsilon<s<0}\,\Phi_s(A)) = \bar{m}_1(\,\cup_{0<s<\varepsilon}\,\Phi_s(F(A)))\ .$$

We leave this as a calculus exercise.

4.1.2 Coupling to neighbors and heat baths

We now consider a chain of N identical copies of the dynamical system described in Sect. 4.1.1, and define couplings between nearest neighbors and between end cells and heat baths.

Let γ_{L} and γ_{R} be two marked subsegments of $\partial\Gamma_0$ of equal length; these segments will serve as openings to allow tracers to pass between cells. For now it is best to think of Γ_0 as having a left-right symmetry, and to think of γ_{L} and γ_{R} as vertical and symmetrically placed (as in Fig. 2), although as we will see, these geometric details are not relevant for the derivation of mean energy and tracer profiles. We call the segments γ_{L} and γ_{R} in the ith cell $\gamma_{\mathrm{L}}^{(i)}$ and $\gamma_{\mathrm{R}}^{(i)}$. For $i = 1, \ldots, N-1$, we identify $\gamma_{\mathrm{R}}^{(i)}$ with $\gamma_{\mathrm{L}}^{(i+1)}$, that is to say, we think of the domains of the ith cell and the $(i+1)$st cell as having a wall in common, namely $\gamma_{\mathrm{R}}^{(i)}$ and $\gamma_{\mathrm{L}}^{(i+1)}$, and *remove* this wall, so that tracers that would have collided with it simply continue in a straight line into the adjacent cell. (See Fig. 2.)

Tracers are injected into the system as follows. Consider, for example, the bath on the left. We say the injection rate is ϱ if at the ring of an exponential clock of rate ϱ, a single tracer enters cell 1 via $\gamma_{\mathrm{L}}^{(1)}$. (Note that the rate ϱ is not the injection rate per unit length of the opening $\gamma_{\mathrm{L}}^{(1)}$ but *per unit time*.) The points of entry and velocities of entering tracers are *iid*, the law being the one governing

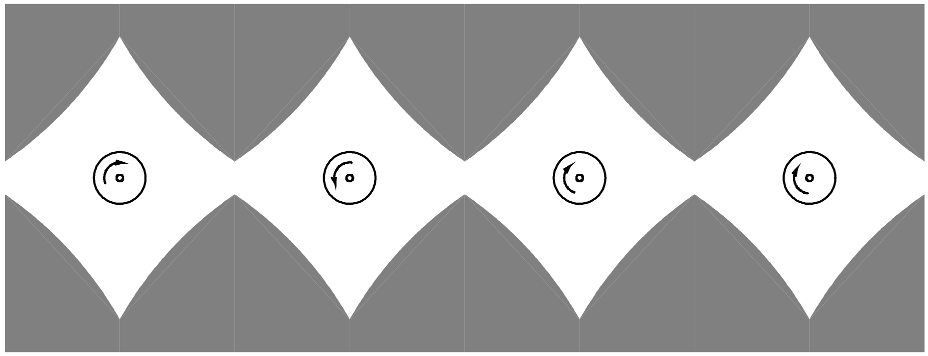

Figure 2: A row of diamond-shaped boxes with small lateral holes (made by removing vertical walls corresponding to $\gamma_{\rm R}^{(i)} = \gamma_{\rm L}^{(i+1)}$) to allow the tracers to go from one box to the next. The shapes of the "boxes" can be quite general for much of our theory. The configuration shown is the one used in the simulations discussed in Sect. 4.5, but with larger holes for better visibility.

the collisions of tracers with $\gamma_{\rm L}^{(1)}$. That is to say, the point of entry is uniformly distributed on $\gamma_{\rm L}^{(1)}$, and the velocity v has density

$$c\, e^{-\beta|v|^2}\, |v||\sin(\varphi)|\; dv\;, \qquad c = \frac{2\beta^{3/2}}{\sqrt{\pi}}\;, \tag{4.14}$$

where $v \in \mathbb{R}^2$ points into $\gamma_{\rm L}^{(1)}$ and $\varphi \in (0,\pi)$ is the angle v makes with $\gamma_{\rm L}^{(1)}$ at the point of entry. (This is the distribution of v at collisions for particles with velocity distribution $\frac{\beta}{\pi}\exp(-\beta|v|^2)dv$.) Here $\beta = 1/T$ where T is said to be the temperature of the bath. Observe that the mean energy of the tracers injected into the system by a bath at temperature T is not T but $3T/2$. Injection from the right is done similarly, via the opening $\gamma_{\rm R}^{(N)}$. When a tracer in the chain reaches $\gamma_{\rm L}^{(1)}$ or $\gamma_{\rm R}^{(N)}$, it vanishes into the baths.

This completes the description of our models. We remark that the process above is a Markov process in which the only randomness comes from the action of the baths. Once a tracer is in the system, its motion is governed by rules that are entirely deterministic.

4.2 Single-cell analysis

In analogy with Sect. 3.2, we investigate in this subsection the invariant measure for a single cell coupled to two heat baths with parameters T and ϱ.

Let $\bar\Omega_k$ and $\bar\Omega_{k,E}$ be as in Sect. 4.1.1. As before, a state of this system is represented by a point in

$$\Omega \;=\; \cup_{k=0}^{\infty}\Omega_k \;=\; \cup_{k=0}^{\infty} \cup_{E\geq 0} \Omega_{k,E}$$

where Ω_k and $\Omega_{k,E}$ are quotients of $\bar\Omega_k$ and $\bar\Omega_{k,E}$ respectively obtained by identifying permutations of the k tracers. With $\{\cdots\}$ representing unordered sets as before, points in Ω are denoted by $z = (\{x_1,\ldots,x_k\},\vartheta;\{v_1,\ldots,v_k\},\omega)$ or simply $(\{x_\ell\},\vartheta;\{v_\ell\},\omega)$, with v_ℓ understood to be attached to x_ℓ. The quotient measures of $\bar m_k$ and $\bar m_{k,E}$ are respectively m_k and $m_{k,E}$.

Abusing notation slightly, we continue to use $\bar\Phi_s$ to denote the semi-flow on $\bar\Omega$, and let Φ_s denote the induced semi-flow on Ω. Then Φ_s is as in Sect. 4.1.1 except where tracers exit or enter the system. More precisely, if $\Phi_s(z) \in \Omega_k$ for all $0 \le s < s_0$, and a tracer exits the system at time s_0, then $\Phi_{s_0}(z)$ jumps to Ω_{k-1}. Similarly, if a tracer is injected from one of the baths at time s_0, then instantaneously $\Phi_{s_0}(z)$ jumps to Ω_{k+1}, the destination being given by a probability distribution.

Let $|\gamma|$ denote the length of the segment γ_{L} or γ_{R}.

Proposition 4.1 *There is an invariant probability measure μ with the following properties:*

(a) the number of tracers present is a Poisson random variable with mean $\varkappa$ where

$$\varkappa = 2\sqrt{\pi}\,\frac{\lambda_2(\Gamma)}{|\gamma|}\,\frac{\varrho}{\sqrt{T}}\ ;$$

(b) the conditional density of μ on Ω_k is $c_k \sigma_k dm_k$ where

$$\sigma_k(\{x_\ell\}, \vartheta; \{v_\ell\}, \omega) \ = \ e^{-\beta(\omega^2 + \sum_{\ell=1}^{k} |v_\ell|^2)}$$

and c_k is the normalizing constant.

We observe as before that the Poisson parameter $\varkappa$ is proportional to ϱ (the higher the injection rate, the more tracers in the cell) and inversely proportional to $\sqrt{T}$, *i.e.*, the speed of the tracers (the faster the tracers, the sooner they leave). Unlike the models considered in Sect. 3, where the tracers are assumed to leave the cell at a rate equal to their speed, here the ratio $\lambda_2(\Gamma)/|\gamma|$ appears, as it should: the smaller the passage way, the longer it takes for the tracers to leave.

Notice that we have not claimed that μ is unique.

We introduce some notation in preparation for the proof. For $A \subset \Omega_k$ and $h > 0$, we let $\Phi_{-h}(A)$ denote the set of all initial states in Ω that in time h evolve into A *assuming no new tracers are injected into the system between times* 0 *and* h.[2] Then $\Phi_{-h}(A) = \cup_{n \ge 0} \Phi^{(n)}_{-h}(A)$ where $\Phi^{(n)}_{-h}(A) = \Phi_{-h}(A) \cap \Omega_{k+n}$, *i.e.*, $\Phi^{(n)}_{-h}(A)$ is the set of states where initially $k+n$ tracers are present, and by the end of time h exactly n of these tracers have exited and the remaining k are described by a state in A.

Lemma 4.2 *Let μ be as in Proposition 4.1, and let A_ε be a cube of sides ε in Ω_k, ε small enough that $\mu(A_\varepsilon) \approx p_k c_k \sigma_k(\bar z)\varepsilon^{4k+2}$ for some $\bar z$. We assume the following holds for all small $h > 0$:*

(i) no tracers are injected into the system on the time interval $(0, h]$;

(ii) $\Phi_h(\Phi^{(0)}_{-h}(A_\varepsilon)) = A_\varepsilon$.

Then

$$\mu(\Phi_{-h}(A_\varepsilon)) \ = \ \sigma_k(\bar z)\varepsilon^{4k+2}\left(p_k c_k + 2h\frac{|\gamma|}{c} p_{k+1} c_{k+1} \ + \ o(h)\right) \tag{4.15}$$

where $p_k = \mu(\Omega_k)$ and $c = \frac{2}{\sqrt{\pi}}\beta^{3/2}$.

Proof: The idea is that for a particle to exit in the very short time h, it must be close to the exit γ_{L} or γ_{R} and move towards it without colliding with the disk or the boundary, *or* it must have very large speed (and that is improbable).

[2] Notice that (1) $\{\Phi_h, h \ge 0\}$ is a semi-flow, and Φ_{-h} is not defined; (2) $\Phi_{-h}(A)$ as defined is $\neq (\Phi_h)^{-1}(A)$.

By assumption (i), we have $\mu(\Phi_{-h}(A_\varepsilon)) = \sum_{n\geq 0} \mu(\Phi_{-h}^{(n)}(A_\varepsilon))$. The $n = 0$ term is handled easily: By virtue of (i) and (ii), the situation is equivalent to that in Sect. 4.1.1. Since $\mu|_{\Omega_k}$ is invariant for the closed dynamical system with k tracers, we have $\mu(\Phi_{-h}^{(0)}(A_\varepsilon)) = \mu(A_\varepsilon)$.

Consider next $n = 1$. We give the estimate for $\mu(\Phi_{-h}^{(1)}(A_\varepsilon))$ assuming $\gamma_{\rm L}$ and $\gamma_{\rm R}$ are straight-line segments, leaving the general case (where these segments may be curved) to the reader. First some notation: For $v \in \mathbb{R}^2$ and $a > 0$, let $E(v, a, {\rm L})$ be the parallelogram on the same side of $\gamma_{\rm L}$ as Γ and with the property that one of its sides is $\gamma_{\rm L}$ while the other is parallel to v and has length a; $E(v, a, {\rm R})$ is defined similarly. To simplify the discussion, we assume that for $a > 0$ sufficiently small, $E(v, a, {\rm L})$ and $E(v, a, {\rm R})$ are contained in Γ, and leave to the reader the verification that "corners" at the end of $\gamma_{\rm L}$ or $\gamma_{\rm R}$ lead to higher order terms (in the variable h used below).

Starting from a state in $\Phi_{-h}^{(1)}(A_\varepsilon)$, we let x and v denote the initial position and velocity of the tracer that exits before time h, and treat separately the cases (1) $|v| \leq \frac{a}{h}$ and (2) $|v| > \frac{a}{h}$. In Case (1), in order for the tracer to exit before time h, we must have $x \in E(v, h|v|, {\rm L}) \cup E(v, h|v|, {\rm R})$, and v must point toward the exits. Since $\lambda_2(E(v, h|v|, {\rm L})) = \lambda_2(E(v, h|v|, {\rm R})) = h|v||\sin(\varphi)||\gamma|$ where φ is the angle v makes with $\gamma_{\rm L}$ or $\gamma_{\rm R}$, we obtain

$$\begin{aligned}\mu(\Phi_{-h}^{(1)}(A_\varepsilon) \cap \{|v| \leq \frac{a}{h}\}) &= \sigma_k(\bar{z})\varepsilon^{4k+2} p_{k+1} c_{k+1} \cdot 2h|\gamma| \int_0^\pi d\varphi |\sin(\varphi)| \int_{|v|\leq \frac{a}{h}} dv |v| e^{-\beta|v|^2} \\ &= \sigma_k(\bar{z})\varepsilon^{4k+2} p_{k+1} c_{k+1} \cdot 2h|\gamma| \frac{1}{c}(1 + o(h))\end{aligned}$$

with $c = 2\beta^{3/2}/\sqrt{\pi}$. For Case (2), we have the trivial estimate $\sigma_k(\bar{z})\varepsilon^{4k+2} p_{k+1} c_{k+1} \cdot o(h)$.

To see that the terms corresponding to $n > 1$ are negligible, we first derive the bound

$$\mu(\Phi_{-h}^{(n)}(A)) \;\leq\; \sigma_k(\bar{z})\varepsilon^{4k+2} p_{k+n} c_{k+n} \, (2h|\gamma|\frac{1}{c} + o(h))^n \, . \tag{4.16}$$

Then we compute the growth rate of $p_{k+n}c_{k+n}$. By the definitions of these numbers, we have

$$\frac{c_{k+1}}{c_k} \cdot \frac{p_{k+1}}{p_k} \;=\; \left(\frac{\lambda_2(\Gamma)}{k+1} \int_{\mathbb{R}^2} e^{-\beta|v|^2} dv \right)^{-1} \left(\frac{1}{k+1} \, 2\sqrt{\pi} \frac{\lambda_2(\Gamma)}{|\gamma|} \frac{\varrho}{\sqrt{T}} \right) ,$$

giving

$$p_{k+n} c_{k+n} \;=\; \left(\frac{c\varrho}{|\gamma|} \right)^n \, p_k c_k, \qquad n \geq 1 \, . \tag{4.17}$$

From (4.16) and (4.17) it follows that $\mu(\Phi_{-h}^{(n)}(A)) \leq \sigma_k(\bar{z})\varepsilon^{4k+2}(\text{const.} \cdot h)^n$.

The asserted bound (4.15) for $\mu(\Phi_{-h}(A))$ is proved. □

The main difference between the proofs of Propositions 3.5 and 4.1 is that Hamiltonian models have both geometry and memory. In preparation for the proof, we introduce the following language. Let A_ε be as in Lemma 4.2. For $\ell = 1, \ldots, k$, we let X_ℓ denote the projection of A_ε onto the plane of its x_ℓ-coordinate, and V_ℓ the projection of A_ε onto the plane of its v_ℓ-coordinate (so that X_ℓ and V_ℓ are ε-squares in Γ and $\mathbb{R}^2$ respectively). We assume for simplicity that for each ℓ, either X_ℓ is a strictly positive distance from $\gamma_{\rm L}$ and $\gamma_{\rm R}$, in which case we say X_ℓ is *in the interior*, or one of its sides is contained in $\gamma_{\rm L}$ or $\gamma_{\rm R}$. In the latter case, we say X_ℓ is *adjacent to an exit*. We further assume that if X_ℓ is adjacent to an exit, then either all $v_\ell \in V_\ell$ point toward the exit or away from it.

Proof of Proposition 4.1: The invariance of μ is already noted in Sect. 4.1.1 except where it pertains to entrances and exits of tracers. We focus therefore on these events, noting that the probability of more than one tracer entering on the time interval $(0,h)$ is $o(h)$, as is the probability of a tracer entering and leaving (immediately) on this time interval. These scenarios will be ignored.

Let A_ε be as above. We seek to show as before that $\frac{d}{dh}\int I_{A_\varepsilon}(z')P^h(dz'|z)\mu(dz)|_{h=0} = 0$. Here it is necessary to treat separately the following configurations for A_ε:

Case 1. The following holds for all ℓ: X_ℓ can be in the interior or adjacent to an exit, and if it is adjacent to an exit, then all v_ℓ in V_ℓ must point toward the exit. Notice that this configuration is relatively inaccessible, meaning the probability of a new tracer entering on $(0,h)$ leading to a state in A_ε is $o(h)\mu(A_\varepsilon)$. Notice also that this configuration has the property $\Phi_h(\Phi^{(0)}_{-h}(A_\varepsilon)) = A_\varepsilon$, so that the contribution of the no-new-tracers event to $\int I_{A_\varepsilon}(z')P^h(dz'|z)\mu(dz)$ is, by Lemma 4.2,

$$\begin{aligned}
&(1-h\varrho)^2\ \sigma_k(\bar z)\varepsilon^{4k+2}\ (p_kc_k + 2h|\gamma|\frac{1}{c}p_{k+1}c_{k+1} + o(h))\\
&= \sigma_k(\bar z)\varepsilon^{4k+2}\ \left(p_kc_k(1-2h\varrho) + 2h|\gamma|\frac{1}{c}p_{k+1}c_{k+1} + o(h)\right)\\
&= \sigma_k(\bar z)\varepsilon^{4k+2}\ (p_kc_k + o(h))\ ,
\end{aligned} \tag{4.18}$$

the last equality being valid on account of Eq. (4.17).

Case 2. X_1 is adjacent to an exit and v_1 points away from it; X_ℓ and V_ℓ for $\ell > 1$ are as in Case 1. In this configuration, there is a part of X_1 that can only be reached in time h if one starts from outside. This region is a parallelogram similar to that in the proof of Lemma 4.2 but with one of its sides equal to $X_1 \cap \gamma_{\rm L}$ or $X_1 \cap \gamma_{\rm R}$. Following the estimates in Case 1, we obtain that the contribution of the no-new-tracers event to $\int I_{A_\varepsilon}(z')P^h(dz'|z)\mu(dz)$ in this case is

$$\sigma_k(\bar z)\varepsilon^{4k+2}\ p_kc_k\left(1 - \frac{h}{\varepsilon}|\bar v_1||\sin(\bar\varphi_1)| + o(h)\right) \tag{4.19}$$

where $\bar v_1$ is the v_1 coordinate of $\bar z$ and $\bar\varphi_1$ is the angle $\bar v_1$ makes with $\gamma_{\rm L}$ (or $\gamma_{\rm R}$).

We now argue that the negative term above is balanced by the contribution of the event in which a new tracer enters on the time interval $(0,h)$. This new tracer must have $v_1 \in V_1$ and must enter through the ε-segment $X_1 \cap \gamma_{\rm L}$ or $X_1 \cap \gamma_{\rm R}$. We claim that the probability of this event is

$$p_{k-1}c_{k-1}\sigma_k(\bar z)e^{\beta|\bar v_1|^2}\varepsilon^{4k-2}\ \cdot\ \varrho h\frac{\varepsilon}{|\gamma|}\ \cdot\ c|\sin(\bar\varphi_1)||\bar v_1|e^{-\beta|\bar v_1|^2}\varepsilon^2\ . \tag{4.20}$$

The first factor in (4.20) is the μ-measure of the states corresponding to those in A_ε but *without* the tracer with position and velocity (x_1, v_1); the second factor is the probability of a tracer entering through the designated segment, and the third is the fraction of tracers entering with velocity $\in V_1$ (see (4.14)). That (4.19) and (4.20) add up to $\mu(A_\varepsilon)(1 + o(h))$ again follows from (4.17).

Case 3. X_1 and X_2 are adjacent to exits, v_1 and v_2 point away from the exits in question, and X_ℓ and V_ℓ are as in Case 1 for $\ell > 2$. We assume for simplicity that either $(X_1 \times V_1) \cap (X_2 \times V_2) = \emptyset$ or $X_1 \times V_1 = X_2 \times V_2$.

In the case $(X_1 \times V_1) \cap (X_2 \times V_2) = \emptyset$, the contribution of the no-new-tracers event is

$$\sigma_k(\bar{z})\varepsilon^{4k+2}\, p_k c_k \left(1 - \frac{h}{\varepsilon}|\bar{v}_1||\sin(\bar{\varphi}_1)| - \frac{h}{\varepsilon}|\bar{v}_2||\sin(\bar{\varphi}_2)| + o(h)\right) , \tag{4.21}$$

and this is cancelled perfectly by the estimate corresponding to (4.20).

In the case $X_1 \times V_1 = X_2 \times V_2$, on $\bar{\Omega}_k$, where tracer positions and velocities are regarded as ordered k-tuples, the set of states where both (x_1, v_1) and (x_2, v_2) are not reachable in time h is $o(h)$, and the set where exactly one of these is not reachable is the union of two sets that project to the same set under π_k. Thus the estimates for both cases are as in Case 2.

The remaining cases are handled similarly. □

Proposition 4.3 *For the N-chain defined in Sect. 4.1.2 with $T_{\mathrm{L}} = T_{\mathrm{R}} = T$ and $\varrho_{\mathrm{L}} = \varrho_{\mathrm{R}} = \varrho$, the N-fold product $\mu \times \cdots \times \mu$ is invariant.*

It suffices to check that the transfer of energy from one cell to the next leads to the correct relation between $p_k c_k$ and $p_{k+1} c_{k+1}$. The proof is left to the reader.

4.3 Derivation of equations of macroscopic profiles

Having found the candidate family of Gibbs measures $\{\mu^{T,\varrho}\}$, we now proceed as in Sect. 3.3, seeking to derive the relevant macroscopic profiles under Assumptions 1 and 2; see Sect. 3.3. There are two new problems, leading to two additional assumptions which we now discuss.

The first problem is that of uniqueness and ergodicity. Unlike their stochastic counterparts, the Hamiltonian chains defined in Sect. 4.1 may not be ergodic; they are, in fact, easily shown to be nonergodic for certain choices of Γ_0. Without ergodicity, it is not clear how to make sense of the notion of *local temperature*, which lies at the heart of Assumption 2. Postponing a discussion to Section 4.4, we bypass this issue by introducing

> **Assumption 1'.** *We assume μ_N is the unique invariant probability measure for the N-chain defined in Sect. 4.1. It follows that μ_N is ergodic.*

Another important departure from the stochastic case is that in Hamiltonian models, local rules are purely dynamical: whether a tracer goes to the left or to the right when it exits a cell is determined entirely by local conditions at the time. In the presence of a nonzero temperature gradient, exit distributions are typically asymmetric in the finite chain, and may depend on specific characteristics of the model in question (see below). We first state a general result giving the relation among the various quantities of interest.

Let $j_{N,i}$ and $Q_{N,i}$ denote respectively the mean number of exits and mean total energy transported out of the ith cell per unit time in the N-chain.

> **Assumption 3.** *We assume that as $N \to \infty$, the profiles $j_{N,i}$ and $Q_{N,i}$ converge in the $\mathcal{C}^0$ sense to functions $j(\xi)$ and $Q(\xi)$ on $(0, 1)$.*

Theorem 4.4 *Under Assumptions 1, 1', 2 and 3, the following hold for the models in Sect. 4.1.*

- *mean stored energy at a site :*
$$s(\xi) \;=\; \frac{1}{3}\,\frac{Q(\xi)}{j(\xi)}\;;$$
- *mean tracer energy :* $e(\xi) = 2s(\xi)$;
- *mean number of tracers :*
$$\varkappa(\xi) \;=\; \frac{\lambda_2(\Gamma)}{|\gamma|}\,\sqrt{\frac{\pi}{2s(\xi)}}\;j(\xi)$$
where $|\gamma| = |\gamma_{\rm L}| = |\gamma_{\rm R}|$ *is the size of the passage between adjacent cells*;
- *mean total-cell energy :*
$$E(\xi) \;=\; s(\xi) + \varkappa(\xi)e(\xi) \;=\; s(\xi) + \frac{\lambda_2(\Gamma)}{|\gamma|}\sqrt{2\pi s(\xi)}\;j(\xi)\;.$$

Proof: The proof follows that of Theorem 3.9, except that all quantities here are expressed in terms of the two functions j and Q (which vary from model to model).

First we read off the pertinent information from Proposition 4.1 for a single cell connected to two heat baths with parameters T and ϱ:

(i) stored energy has density $\frac{\sqrt{\beta}}{\sqrt{\pi y}}e^{-\beta y}$ and mean $s = \frac{T}{2}$;
(ii) tracer energy has density $\beta e^{-\beta x}$ and mean T ;[3]
(iii) mean number of tracers, $\varkappa = \frac{\lambda_2(\Gamma)}{|\gamma|}\sqrt{\pi}\frac{2\varrho}{\sqrt{T}}$;
(iv) mean total-cell energy, $E = T(\varkappa + \frac{1}{2})$;
(v) mean number of jumps out of cell per unit time, $j = 2\varrho$;
(vi) mean total energy transported out of cell per unit time, $Q = \frac{3T}{2}\cdot j = 3T\varrho$.

To prove (i), for example, we condition on the event that exactly k tracers are present. Integrating out all other variables, we obtain that the distribution of ω is $\mathrm{const}.e^{-\beta\omega^2}$. Thus the distribution of $s = \omega^2$ is as claimed. Items (ii) – (iv) are proved similarly, and (v) and (vi) are deduced from the fact that the cell is in equilibrium with the two baths.

To deduce the asserted profiles, fix $\xi \in (0,1)$, and consider the $[\xi N]$-th cell in the N-chain. By Assumption 2, $\mu_{N,[\xi N]} \to \mu^{T(\xi),\varrho(\xi)}$ for some $T(\xi)$ and $\varrho(\xi)$. Moreover, with respect to this limiting distribution, the number of jumps per unit time out of the cell is $j(\xi)$, and the total energy transported out of the cell is $Q(\xi)$. We then use the single-cell information above combined with these values of $j(\xi)$ and $Q(\xi)$ to identify $T(\xi)$ and $\varrho(\xi)$. The formula for s is obtained as follows: $T = \frac{2}{3}Q/j$ is from (v) and (vi), and $s = \frac{1}{2}T$ is from (i). □

Of particular interest to us are models in which there is good mixing *within individual cells*. In an idealized model in which mixing within individual cells is perfect and instantaneous, exits to the left and the right would be equally likely, as would be the case for mean energy flow. With such a perfect left-right symmetry at each site, j and Q would be linear as explained in the proof of Theorem 3.9. For the class of models described in Sect. 4.1, this idealized state is never attained, but we have found that exit distributions come very close to being symmetric under certain conditions:

[3]Note that this is the energy density when the tracers are *in the box*, to be distinguished from (vi).

The most important of these conditions are (i) a geometry of Γ_0 that gives rise to fast mixing for the closed dynamical system (such as concave walls and the absence of "traps"), and (ii) small passageways between adjacent cells (so most tracers stay in the cell for a long time). The presence of large numbers of tracers is also conducive to good mixing. [4]

Corollary 4.5 *In the setting of Theorem 4.4, if j and Q have approximately linear profiles with $j(0) = \varrho_{\rm L}, j(1) = \varrho_{\rm R}, Q(0) = T_{\rm L}\varrho_{\rm L}$ and $Q(1) = T_{\rm R}\varrho_{\rm R}$, then the profile for mean stored energy is given by*

$$s(\xi) \;\approx\; \frac{1}{2}\frac{\varrho_{\rm L}T_{\rm L} + (\varrho_{\rm R}T_{\rm R} - \varrho_{\rm L}T_{\rm L})\xi}{\varrho_{\rm L} + (\varrho_{\rm R} - \varrho_{\rm L})\xi}\ .$$

Other approximate profiles are obtained similarly by substituting

$$j(\xi) \;\approx\; 2\,(\varrho_{\rm L} + (\varrho_{\rm R} - \varrho_{\rm L})\xi)$$

into the formulas in Theorem 4.4.

Numerical simulations validate these predictions for Hamiltonian chains with small passageways between cells. See Sect. 4.5. Our findings suggest, in fact, $\mathcal{C}^2$ convergences to j and Q. More precisely, let $j_{N,i} = j_{N,i,{\rm L}} + j_{N,i,{\rm R}}$ where $j_{N,i,{\rm L}}$ and $j_{N,i,{\rm R}}$ are the numbers of exits per unit time that go to the $(i-1)$st and $(i+1)$st cells respectively. Analogously, let $Q_{N,i} = Q_{N,i,{\rm L}} + Q_{N,i,{\rm R}}$. Then for each compact set of cell configurations $(\Gamma_0, \gamma_{\rm L}, \gamma_{\rm R})$ and parameters $T_{\rm L}, T_{\rm R}, \varrho_{\rm L}, \varrho_{\rm R} > 0$, there exists an $\alpha \geq 0$ such that for all large N, the following hold for all i:

$$|j_{N,i,{\rm R}} - \frac{1}{2}j_{N,i}| \leq \frac{\alpha}{N}\ ; \quad |Q_{N,i,{\rm R}} - \frac{1}{2}Q_{N,i}| \leq \frac{\alpha}{N}\ ;$$
$$|(j_{N,i,{\rm R}} - \frac{1}{2}j_{N,i}) - (j_{N,i+1,{\rm R}} - \frac{1}{2}j_{N,i+1})| \leq \frac{\alpha}{N^2}\ ;$$
$$|(Q_{N,i,{\rm R}} - \frac{1}{2}Q_{N,i}) - (Q_{N,i+1,{\rm R}} - \frac{1}{2}Q_{N,i+1})| \leq \frac{\alpha}{N^2}\ .$$

The situation in Corollary 4.5 corresponds to the case $\alpha \ll 1$.

Remark 4.6 The bounds above are consistent with the following observations: For a cell in the N-chain, the temperature difference between the cell on its left and the one on its right is of order $|T_{\rm L} - T_{\rm R}|/N$, so one expects the marginal of μ_N at this site to deviate from the equilibrium measure in Sect 4.2 by the same order of magnitude. This deviation is in turn reflected in the differences $|j_{N,i,{\rm R}} - j_{N,i,{\rm L}}|$ and $|Q_{N,i,{\rm R}} - Q_{N,i,{\rm L}}|$. Similarly, if the second differences are well behaved as we assume, their orders of magnitude as indicated above are dimensionally correct. Detailed dependencies of this asymmetry on the physical parameters are beyond the scope of this paper.[5]

The discussion of results in Sect. 3.5 (with "linearity" replaced by "approximate linearity") applies to models satisfying the hypotheses in Corollary 4.5. Statements not involving linearity of j and Q apply to the broader setting of Theorem 4.4.

[4]It is important to distinguish between the following two levels of mixing: mixing *within cells*, and mixing *in the chain*. For example, small passageways between cells enhance mixing of the first kind but are obstructions to the latter.

[5]We thank H. Spohn for interesting correspondence on this point.

4.3.1 Comparisons of models

1. *Predicted profiles for Hamiltonian and stochastic models.* We observe that the predicted formulas in Theorem 4.4 are of the same type as their counterparts in Theorem 3.9 but the constants are different. The similarity stems from the fact that they are derived from the same general principles. The differences in constants reflect the differences in $\mu^{T,\varrho}$, which in turn reflect the differences in local rules (see below).

2. *Relation between s and e.* To highlight the role of the local rules in the profiles studied in this paper, we recall the relation between stored energy s and individual tracer energy in the various models encountered:

(a) Random halves (Sects. 3.1–3.3): $s = 2e$. (At collisions, energy is split evenly on average, but the expected time for the next clock is longer for slower tracers.)
(b) Stochastic models simulating Hamiltonian systems where both disk and tracer have a single degree of freedom (Sect. 3.6): $s = e$.
(c) Hamiltonian models in which the disk has one degree of freedom and tracers have two (Section 4.1): $e = 2s$.

To this list, we now add one more example, namely

(d) Hamiltonian models in which the disk has one degree of freedom and tracers have 3: Consider the model described in Sect. 4.1, but with $\Gamma_0 \subset \mathbb{R}^3$ and the disk replaced by a cylinder that rotates along a fixed axis. Here, Liouville measure for a closed system with k tracers is $\bar{m}_k = (\lambda_3|_\Gamma)^k \times (\nu_1|_{\partial D}) \times \lambda_{3k+1}$ (*cf.* Sect. 4.1.1). From a single-cell analysis similar to that in Sect. 4.2, $\mu^{T,\varrho}$ is easily computed. One notes in particular that the distribution of tracer energy is $\text{const.}\sqrt{x}e^{-\beta x}$, while disk energy is as before. A simple computation then gives $e = 3s$.

These examples demonstrate clearly that the relation between s and e is entirely a function of the local structure. In the case of Hamiltonian systems, we see that it is also dimension-dependent.

4.4 Ergodicity issues

Questions of ergodicity for the chains in Theorem 4.4 are beyond the scope of this paper. We include only brief discussions of the following three aspects of the problem:

1. Randomness in the injection process

Among the various features of our models, the one the most responsible for promoting ergodicity is the randomness with which new tracers are injected into the system. We observe, however, that this genuinely stochastic behavior occurs only at the two ends of the chain, and even there, the transition probabilities do not have densities with respect to the underlying Lebesgue measure. The problem is thus one of *controllability* involving the deterministic part of the dynamics.

2. Hyperbolicity of billiard dynamics: a necessary condition

Let $\Delta_N \subset \mathbb{R}^2$ denote the playground for the tracers in the N-chain. That is to say, it is the union of N copies of Γ arranged in the configuration shown in Fig. 2 with open passages between adjacent copies of Γ. The presence of one of more tracers being *trapped* in Δ_N without contact with any of the turning disks or the openings at the two ends (*i.e.*, $\gamma_{\mathrm{L}}^{(1)}$ and $\gamma_{\mathrm{R}}^{(N)}$) is clearly an obstruction to ergodicity. This scenario is easily ruled out by choosing Γ_0 to have concave (or scattering) walls.

Such a choice of Γ_0 implies that $\partial\Delta_N$ also has concave boundaries, and the free motion of a particle in a domain with concave boundaries is well known to be hyperbolic and ergodic [21, 16].

We do not know if the absence of trapped tracers in the sense above implies ergodicity.

3. Enhancing ergodicity

Without (formally) guaranteeing ergodicity, various measures can be taken to "enhance" it, meaning to make the system appear for practical purposes as close to being ergodic as one wishes. For example, one can introduce more scattering within each cell by increasing the curvature of the walls of Γ_0, or alternately, one could add convex bodies inside Γ_0 that play the role of Lorentz scatterers. Another possibility is to add a small amount of noise, and a third is to increase the injection rates: physical intuition says that the larger the number of tracers in the system, the more likely stored energy will behave ergodically.

4.5 Results of simulations

To check the applicability of the theory proposed in Sects. 4.1–4.3 to real and finite systems, we have done extensive simulations some of which we describe in this subsection. The domain Γ_0 used in our simulations is as shown in Fig. 2. Actual specifications of Γ_0 are as follows: We start with a square of sides 2, subtracting from it first 4 disks of radius 1.15 centered at the 4 corners of the square. Two openings corresponding to γ_{L} and γ_{R} are then created on the left and right; each has length 0.02. This completes the definition of Γ_0. The disk D is located at the center of the square; it has radius $r = 0.0793$.

Our choice of domain was influenced by the following factors: First, $\partial\Gamma_0$ is taken to be piecewise concave to promote ergodicity. Second is the size of the disk: A disk that is too small is hit by a tracer only rarely; many tracers may pass through the cell without interacting with the disk (this is analogous to having a large δ in Sect. 3.1). A disk that is too large (relative to the domain in which it can fit) may cause an unduly large fraction of tracers entering the box to exit immediately from the same side. Both scenarios lead to large time-correlations, which are well known to impede the speed of convergence to μ_N in a finite chain. They may also affect the infinite-volume limit.

We have found the geometry and specifications above to work quite well, with a tracer making, on average, about 71 collisions while in a cell. Of these collisions, about 12.5 are with the disk.

For the single cell (with the geometry above) plugged to two identical heat baths, we have tested the system extensively for ergodicity. To the degree that one can ascertain from simulations, there is an ergodic component covering nearly 100% of the phase space. The various energy distributions as well as the Poisson distribution of the number of tracers present agree perfectly with those predicted by Proposition 4.1.

Simulations for chains of 20 to 60 cells with the choice of r and $|\gamma|$ above showed very good agreement with the theory. A sample of the fits for $Q(\xi)$, $s(\xi)$ and $E(\xi)$ for $9 \cdot 10^9$ events and 30 sites is shown in Figure 3. Here the ejection rates to the left and right are very close to $50/50$. We have also investigated the quantity α toward the end of Sect. 4.3 for various values of r and $|\gamma|$, up to $r = 0.23$ (which is quite close to the maximum-size disk that can be fitted into the domain Γ_0) and $|\gamma| = 0.06$. Our findings are consistent with the discussion in Sect. 4.3.

In addition to these profiles, we have also verified directly Assumption 2, which asserts that the distributions of energy and tracers within each cell are in accordance with those given by $\mu^{T,\varrho}$ for some T, ϱ depending on the cell. A sample of these results is shown in Fig. 4.

4.6 Related models

In this subsection we recall from the literature a few models that in their original or slightly modified form can be regarded as approximate realizations of the class described in Sect. 2.1 of this paper. For more complete accounts, see the review papers [2, 13, 15].

The models which come closest to ours, and which to some degree inspired this work, are those in [17, 12]. In these papers, the authors carried out a numerical study of a system comprised of an array of disks similar to those in Sect. 4.1 but arranged in two rows with periodic boundaries (in the vertical direction). These disks interact via tracers following the rules first used in [20]. We have adopted the same local rules, but have elected to arrange our disks in a single row to simplify the analysis.

There is a number of papers dealing with mechanical gadgets that on some level appear similar to ours. For example, in [14, 9], vertical plates are pushed back and forth by particles trapped between them. The main difference between these models and ours is that they have exactly one "tracer" in each "cell". In this respect, these models are closer to our earlier work [6] in which locked-in tracers were considered. Ding-a-ling and ding-dong models belong essentially to the same class [3, 19, 8, 18].

We mention that nonlinearities of profile are difficult to see when the temperature differences at the two ends are relatively small (in fact, what counts in many cases, including the models studied in this paper, is the *ratio* of temperatures at the two ends). This may explain why some authors have reported linear profiles when our analysis suggests that may not be the case.

We mention also a very well-studied situation, namely that of the Fermi-Pasta-Ulam chain. In this model, and in many others, there is a potential of the form

$$U(x_i - x_{i+1}) + V(x_i) ,$$

with U and V functions that grow to ∞ and x_i the coordinates of a chain of anharmonic oscillators. The pinning potential V plays the role of the "tank" in our models, while the interparticle potential is more akin to the role of the tracers. This class of models is difficult to handle because in contrast to the basic setup in our study, there is no clear separation of the pinning and interaction energies.

Finally, we mention that Hamiltonian systems with noise have been studied in the context of the Fourier Law. See *e.g.* [1].

Acknowledgments: The authors thank O. Lanford for helpful discussions. JPE acknowledges the Courant Institute, and LSY the University of Geneva, for their hospitality.

References

[1] C. Bernardin and S. Olla. Fourier's law for a microscopic model of heat conduction. *Preprint (2005)* .

[2] F. Bonetto, J. L. Lebowitz, and L. Rey-Bellet. Fourier's law: a challenge to theorists. In: *Mathematical physics 2000* (London: Imp. Coll. Press, 2000), pp. 128–150.

[3] G. Casati, J. Ford, F. Vivaldi, and W. Visscher. One-dimensional classical many-body system having a normal thermal conduction. *Phys. Rev. Lett.* **52** (1984), 1861–1864.

[4] S. De Groot and P. Mazur. *Non-Equilibrium Thermodynamics* (North Holland, 1962).

[5] A. De Masi and E. Presutti. *Mathematical methods for hydrodynamic limits*, volume 1501 of *Lecture Notes in Mathematics* (Berlin: Springer-Verlag, 1991).

[6] J.-P. Eckmann and L.-S. Young. Temperature profiles in Hamiltonian heat conduction. *Europhysics Letters* **68** (2004), 790–796.

[7] G. Eyink, J. L. Lebowitz, and H. Spohn. Hydrodynamics of stationary nonequilibrium states for some stochastic lattice gas models. *Comm. Math. Phys.* **132** (1990), 253–283.

[8] P. Garrido, P. Hurtado, and B. Nadrowski. Simple one-dimensional model of heat conduction which obeys fourier's law. *Phys. Rev. Lett.* **86** (2001), 5486–5489.

[9] C. Gruber and A. Lesne. Hamiltonian model of heat conductivity and Fourier law. *Preprint* .

[10] C. Kipnis and C. Landim. *Scaling limits of interacting particle systems*, volume 320 of *Grundlehren der Mathematischen Wissenschaften [Fundamental Principles of Mathematical Sciences]* (Berlin: Springer-Verlag, 1999).

[11] C. Kipnis, C. Marchioro, and E. Presutti. Heat flow in an exactly solvable model. *J. Statist. Phys.* **27** (1982), 65–74.

[12] H. Larralde, F. Leyvraz, and C. Mejía-Monasterio. Transport properties of a modified Lorentz gas. *J. Stat. Phys.* **113** (2003), 197–231.

[13] S. Lepri, R. Livi, and A. Politi. Thermal conduction in classical low-dimensional lattices. *Phys. Rep.* **377** (2003), 1–80.

[14] B. Li, G. Casati, J. Wang, and T. Prosen. Fourier law in the alternate mass hard-core potential chain. *Phys. Rev. Lett.* **92** (2004), 254301.

[15] B. Li, G. Casati, J. Wang, and T. Prosen. Fourier law in the alternate mass hard-core potential chain (cond-mat/0307692).

[16] C. Liverani and M. P. Wojtkowski. Ergodicity in Hamiltonian systems. In: *Dynamics reported*, volume 4 of *Dynam. Report. Expositions Dynam. Systems (N.S.)* (Berlin: Springer, 1995), pp. 130–202.

[17] C. Mejía-Monasterio, H. Larralde, and F. Leyvraz. Coupled normal heat and matter transport in a simple model system. *Phys. Rev. Lett.* **86** (2001), 5417–5420.

[18] H. A. Posch and W. G. Hoover. Heat conduction in one-dimensional chains and nonequilibrium Lyapunov spctrum. *Phys. Rev. E* **58** (1998), 4344–4350.

[19] T. Prosen and M. Robnik. Energy transport and detailed verification of fourier heat law in a chain of colliding harmonic oscillators. *J. Physics. A* **25** (1992), 3449–3478.

[20] K. Rateitschak, R. Klages, and G. Nicolis. Thermostating by deterministic scattering: the periodic Lorentz gas,. *J. Stat. Phys.* **99** (2000), 1339–1364.

[21] J. G. Sinaĭ. Dynamical systems with elastic reflections. Ergodic properties of dispersing billiards. *Uspehi Mat. Nauk* **25** (1970), 141–192.

[22] H. Spohn. *Large Scale Dynamics of Interacting Particles*. Texts and Monographs in Physics (Heidelberg: Springer-Verlag, 1991).

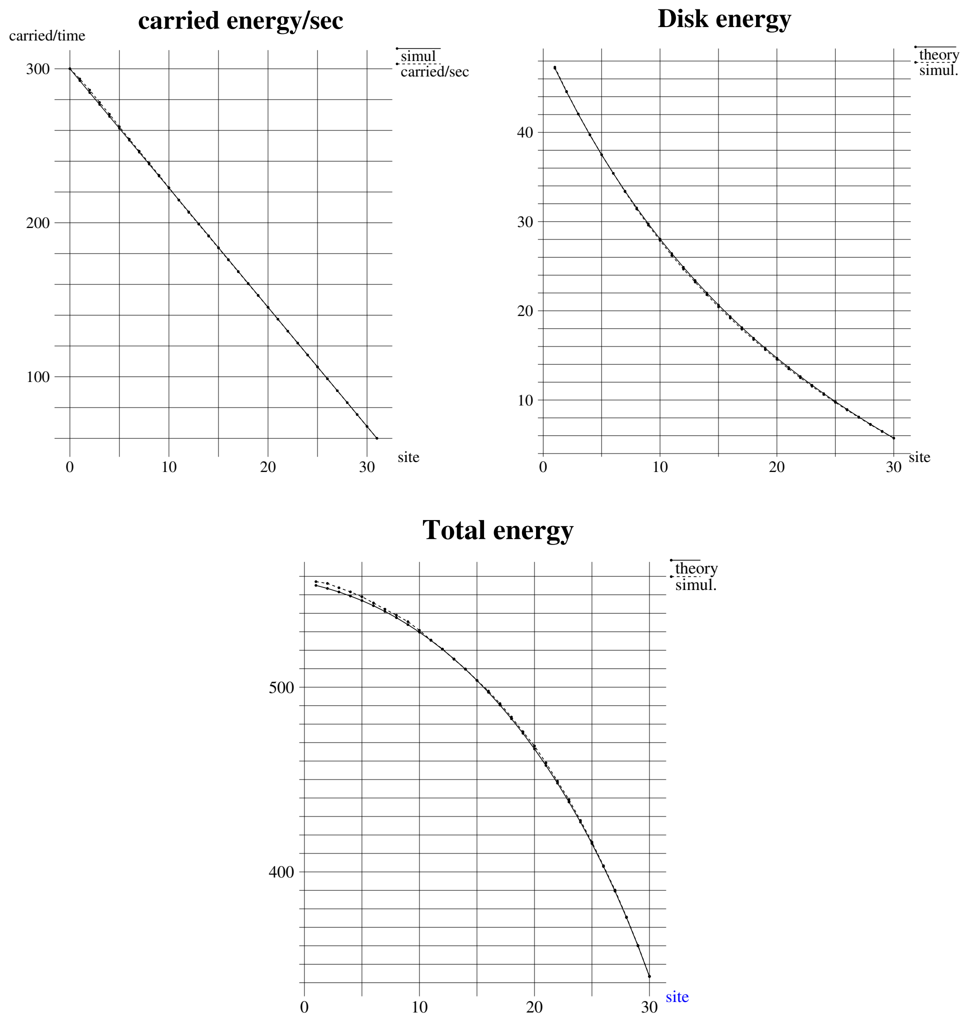

Figure 3: Rotating disks model with chain of 30 cells, temperatures $T_{\mathrm{L}} = 100$, $T_{\mathrm{R}} = 10$, and injection rates $\varrho_{\mathrm{L}} = 1$, $\varrho_{\mathrm{R}} = 2$. Top left: Q_i, energy transported out of site i per unit time as a function of i. Top right: Mean disk energy s_i. Bottom: Mean total energy E_i.

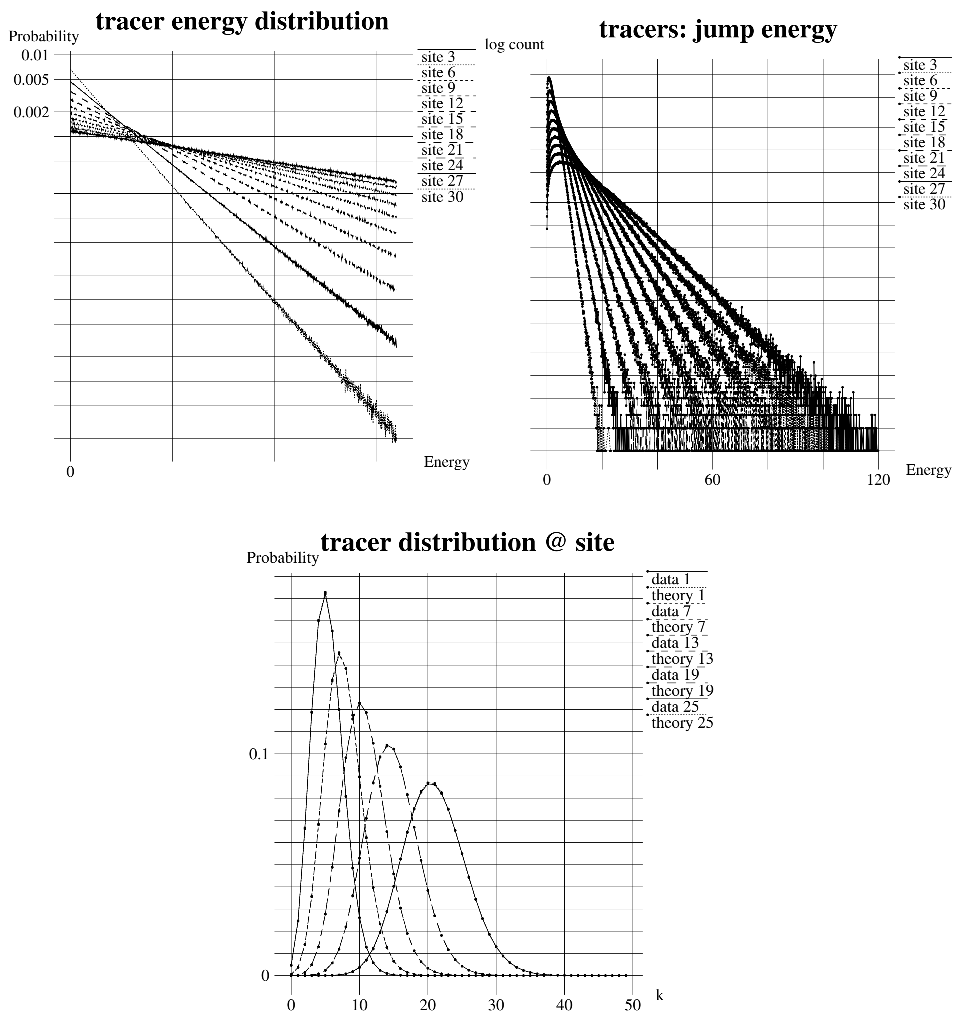

Figure 4: Same parameters as in Fig. 3. Top 2 figures show semi-log plots of tracer energy distributions at various sites. Top left: Densities of tracer energies inside boxes (theory predicts $\beta e^{-\beta x}$). Top right: Densities of tracer energies upon exiting the various boxes (theory predicts $2\beta^{\frac{3}{2}}\sqrt{x/\pi}e^{-\beta x}$). Bottom: Distribution of numbers of tracers at several sites (theory predicts Poisson distribution).